ABSTRACT

The purpose of this work is to study the effect of calcination parameters (temperature and duration) on the structural properties and activity of carbon nanofiber-supported Cu/ZrO_2 ($Cu\text{-}ZrO_2/CNF$) catalyst. The catalyst was prepared by deposition precipitation method with fixed metal loading of 20wt% Cu and 5wt% Zr on CNF and calcined at temperature between 250-550˚C and duration between 3-4 hours. The catalyst structural properties were characterize using Thermal Gravimetric Analysis (TGA), BET analysis, X-ray diffraction (XRD) and Temperature Programmed Reduction (TPR). The performance of the catalysts were studied in a stirred reactor at feed ratio H_2/CO_2 = 3:1, Temperature = 443 K and Pressure =3.0 MPa for 3 hours. XRD studies revealed that the degree of crystallization of catalyst increased with increase of calcination temperature. BET analysis showed that the catalyst subjected to low calcination temperature has higher surface area. TPR analyses concluded that the reduction temperature for the catalyst is 350˚C and suggested that higher temperature and longer duration of calcination give more narrow peak which describe large CuO particle present on the catalyst surface. The highest yield of methanol, 38.67%, was achieved using the catalyst calcined at temperature 550˚C and duration of 4 hours.

ACKNOWLEDGEMENT

Praise to Allah for His guidance and blessings He has given me throughout this Final Year Project. It's the strength from him that it what keeps us going in everything we do. My greatest appreciation goes to my supervisor, Dr. Maizatul Shima Shaharun for helping, teaching, giving advices and opinions through completing this work. I appreciate her efforts and time she allocates for me. Million thanks to her for giving me this opportunity and her confidence in me.

My appreciation also goes to Final Year Project Coordinator, Dr. Norhayati Mellon for her guide and help in ensuring the smoothness of this course. Special thanks to my parents for the continuous. Last but not least, I would like to thank everyone who have involved directly and indirectly in helping me during project execution. Thank you so much.

TABLE OF CONTENTS

LIST OF FIGURES

LIST OF TABLES

CHAPTER 1: STUDY BACKGROUND

1.1. Background Study

Global warming is a very popular issue and has intensively been debated among people in this recent years. It is reported that, the change in climate is caused by man-made emissions of greenhouse gases which reduce the ozone layer that shield earth from sun heat ray. One of the greenhouse gases which is believed to be the major cause in climate change is carbon dioxide. It is reported that the global concentration of carbon dioxide has increase up to 370 ppm (C.D. Keeling, 1997) since the industrial revolution. This trigger the awareness in society to manage and recycle carbon dioxide before it been release into the atmosphere. One way of doing it is by recycling the carbon dioxide to form methanol. This is known as CO_2 hydrogenation process. Methanol is a monohydric alcohol with simple alcohol compound, comprised of one carbon atom, one oxygen atom and hydrogen atom. Methanol is known as a very important chemical derivative that mostly used in chemical industry such as chemical feedstock, antifreeze and green transportation fuel. Due to its nature, methanol has attracted attention as an alternative for energy production which cause increase in demand.

The first commercial methanol synthesis was implemented by BASF in 1923 at high pressure (250-350 bar) and high temperature (320-450˚C) condition which is extremely dangerous. In 1966, ICI develop a more active catalyst which enable methanol to be synthesized at lower temperature and pressure. This accidentally spark and revolutionized the research and development field of methanol synthesis to come out with best performance catalyst that give better yield of methanol at lower operating condition.

1.2. Problem statement

Methanol synthesis from carbon dioxide is known to be an extreme process because it is highly influence by the thermodynamics of the reaction. Current studies found that the hydrogenation of carbon dioxide only yield a small amount of methanol. There are also reported that the reaction of carbon dioxide to methanol exhibit water affinity which reduce the active metal sites of the catalysts used in the process which is known as catalyst poisoning. Thus, reducing the catalyst span life.

It is also known that the yield of methanol is affected by the surface area of the active metal site of the catalyst. In addition, found that the dispersion of the active metal on the catalyst support could affect the performance of the catalyst and the yield of the methanol. Thus, the properties of hydrogenation product can be significantly affected by the activity and structure of the employed catalyst.

1.3. Objectives

The purpose of this study are;

a) To synthesize Cu/ZrO_2 catalyst supported on carbon nanofiber ($Cu\text{-}ZrO_2/CNF$) at different calcination parameters.
b) To correlate calcination parameters to the catalyst structural properties and activity.
c) To test the activity and selectivity of the prepared catalyst in a stirred reactor at fixed reaction condition.
d) To determine the optimum calcination parameters for the prepared $Cu/ZrO_2/CNF$.

1.4. Scope of study

This project will focus on:

a) Synthesis of Carbon Nanofiber (CNF)-supported Cu/ZrO_2 catalyst at different calcination parameters.
b) Determine the activity and selectivity of the prepared catalyst in hydrogenation of CO_2 reaction.
c) Determine the optimum calcination temperature and duration for preparing the $Cu-ZrO_2$/CNF catalyst.

1.5. Feasibility of the project

This project is possible to be carried out because the equipments are available at the place of study and also the materials or information can be found whether in the place of study and online.

CHAPTER 2: LITERATURE REVIEW

2.1. Methanol

Methanol is commonly known as methyl alcohol and abbreviated as MeOH, can be classified as hydrocarbon with chemical formulation of CH_3OH. Methanol was found and used since Ancient Egypt which obtain from the pyrolysis of wood. Methanol is widely used in our lives daily. Examples of applications of methanol (http://www.methanol.org/Methanol-Basics/Methanol-Applications.aspx, 2011) :

a) Transportation fuel: used as fuel that power our car engine.
b) Electricity generation: Some country use methanol as an option for electricity. The combustion of methanol will create stream of steam which drives the turbines.
c) Wastewater denitrification: wastewater contain high concentration of ammonia. the biodegradation process that take place in the water convert ammonia to nitrate. Upon discharged, it will increase the Biochemical Oxygen Demand (BOD) which harm the water ecosystem.

Below is the summarization properties of methanol retrieved from www.methanex.com/methanol/techsafetydata.htm :

Table 1: Physical properties of methanol

Molecular Formula	CH_3OH
Molar mass	32.04g/mol
Appearance	Colorless liquid
Density	0.7918 g/cm³, liquid
Melting Point	–97 °C
Boiling Point	64.7 °C
Solubility in Water	Fully miscible
Acidity (pKa)	~15.5
Viscosity	0.59 mPa·s
Dipole Moment	1.69 D

Methanol is an important chemical that widely used in petrochemical industries. Below are the usage of methanol, market supply and market demand retrieved from http://www.methanolmsa.com/exec/sam/view/id=183/node=115/

Table 2: Usage of methanol

Primary Derivative	Secondary Derivative	Tertiary Derivative	Quaternary Derivative
Acetic Acid	Viny Acetate	Polyvinyl Acetate	Polyvinyl Alcohol
			Ethylene Vinyl Acetate
	Acetic Anhydride	Cellulose Acetate (filter tow)	
	Terephthalic Acid	Polyesters (polyethylene terepthatlate)	
Formaldehyde	Phenol Formaldehyde Resins		
	Urea Formaldehyde Resins		
	Melamine Resins		
	Polyoxymethylene (POM or Polyacetal)		
	Polyols		
	Butanediol	Polyesters (polybutyl terepthalate)	
	Isoprene		
	Paraformaldehyde	rubber (polyisoprene)	
	Hexamine		
Methy tert-butyl ether (MTBE)			
Methyl Methacrylate	Polymethylmethacrylate (PMMA)		
	Methacrylate/Acrylate Co Polymers		
Methyl Chloride (Chloromethane)	Methylene Chloride (CH_2Cl_2)	Chloroform ($CHCl_3$)	Carbon Tetrachloride
Methylamines			
*Monomethyamine	Caffeine (stimulant,diruretic)		
	Sevin/carbaryl (insecticide)		
	Water gel explosives		
	Photographic developers		
	Analgesics (Demerol)		
	Antispasmodics		

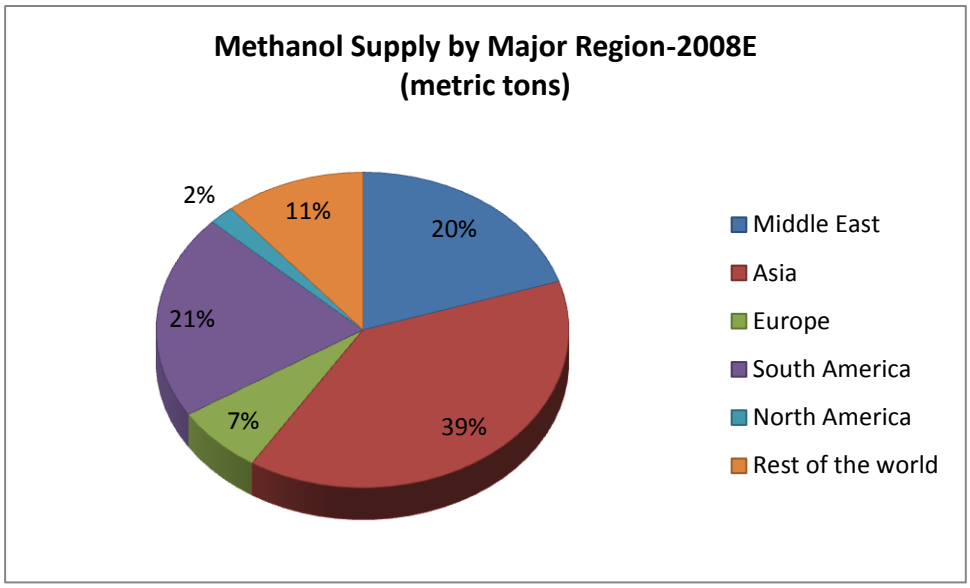

Figure 1: Supply market for methanol

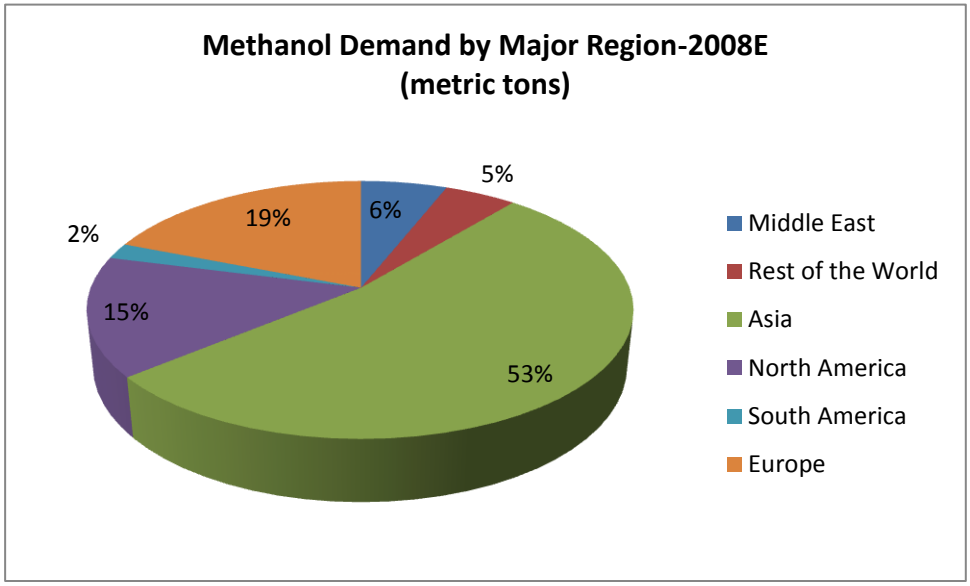

Figure 2: Demand market for methanol

2.2. Methanol synthesis reaction

There are two common steps in methanol synthesis that used in current industry. First is direct oxidation of methane to methanol and second is the conversion of synthesis gas (CO/ CO_2/H_2) to methanol by hydrogenation process. Syngas or synthesis gas is produce from the steam reforming of natural gas or liquid hydrocarbon (Leiviska, December 2008) . Below are the routes for methanol synthesis:

a) Direct oxidation of methane:

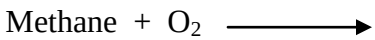

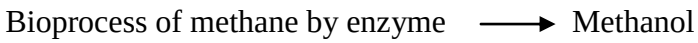

b) Synthetic gas to methanol:

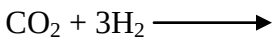

ΔH_{298K}= -49.5 kJ/mol

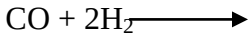

ΔH_{298K}=41.154kJ/mol

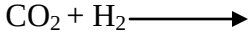

ΔH_{298K}= 41.154 kJ/mol

Through the reaction of synthetic gas to methanol reaction, there is possibility for water gas shift reaction to occur. The reaction is exothermic where the carbon monoxide will reacts with water vapor to form carbon monoxide and hydrogen:

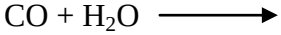

ΔH_{298K}= -41.2 kJ/mol

2.2.1. Methanol synthesis from synthetic gas

Most common practice used for methanol synthesis is by using the synthetic gas ($CO/CO_2/H_2$) that obtain from natural gas reforming. The process is favor by the assist of catalyst. The feed compositions of the methanol synthesis are mainly CO, CO_2 and excess of H_2. Meanwhile the products from the process are methanol and there are some trace of water and methane can be found. Since the process is affected by the performance of catalyst, various of studies have been conducted to determine the mechanism of active sites on the surface species to obtain high yield of methanol.

The synthesis of methanol from synthetic gas is structure from two exothermic reaction.. First is from the water gas shift reaction and secondly is the hydrogenation of CO_2 to methanol. Below are the reactions and enthalpies:

$$CO + H_2O \longrightarrow H_2 + CO_2 \qquad \Delta H_{298K} = -41.2 \text{ kJ/mol}$$

$$CO_2 + 3H_2 \longrightarrow CH_3OH + H_2O \qquad \Delta H_{298K} = -49.5 \text{ kJ/mol}$$

The balance from these two equation will give net conversion of CO to Methanol.

$$CO + 2H_2 \longleftrightarrow CH_3OH \qquad \Delta H_{298K} = 41.154 \text{kJ/mol}$$

Due to thermodynamic of the process that strongly exothermic, the operating condition of the reaction take place at high temperature (250˚C) and high pressure (50-80 atm).

2.2.2. CO_2 hydrogenation to methanol

Due to increase emission of CO_2 especially from large facilities and fossil fuel combustion, various debate among scientist and research study have been conducted in determine the possibility of CO_2 conversion to methanol. CO_2 is a chemical compound that very thermodynamically stable and increase awareness on global climate change encourage to utilize this greenhouse gas more efficiently.

With excess of carbon dioxide available it can be consider as an alternative feedstock to replace CO in the synthesis of methanol. It happens that reverse water gas shift reaction also occurs in CO_2 hydrogenation as in the methanol synthesis from synthetic gas. At the same time, methanol decomposition take place which give high concentration of undesired CO but when react with excess of hydrogen it will result the yield of methanol. Below are the reaction flow:

$$CO_2 + H_2 \longleftrightarrow CO_2 + H_2O \qquad \Delta H_{298K} = 41.154 \text{ kJ/mol}$$

$$CH_3OH \longleftrightarrow CO + 2H_2 \qquad \Delta H_{298K} = 90.6 \text{ kJ/mol}$$

2.3. Catalyst for CO_2 hydrogenation

The hydrogenation of carbon monoxide and carbon dioxide tend to produce higher alcohols over methanol and at the same time form dimethylether in the synthesis process. Various catalysts have been created to allow the production of methanol under gas low pressure condition. These catalysts are Cu-based catalyst with mixture of oxides such as ZnO, ZrO_2 and Al_2O_3.

2.3.1. $Cu/ZnO/Al_2O_3$ catalyst

$Cu/ZnO/Cr_2O_3$ is the first catalyst that been used in industry which was introduced by BASF. But the studies found that the catalyst tend to favor higher alcohol than methanol (Burcham et al., 1998) . Detail studies on the properties of the catalyst found that metallic Cu acts as an active site where methanol synthesis happen (Chinchen et al., 1983). This led to $Cu/ZnO/Al_2O_3$ catalyst that currently used in industry.

The use of $Cu/ZnO/Al_2O_3$ in methanol synthesis is actively debate and widely studied. According to Chinchen et al. (1987) and Sheffer et al. (1989) metallic copper is inactive for the hydrogenation of CO and the promotional of alkali metals affect the stabilization of Cu^+ species.

Function of ZnO is to increase the dispersion of the Cu phase during the preparation of the catalyst which increase the surface area of the Cu. Furthermore, ZnO help to prevent the Cu particles from sintering. Substitution of Zn into Cu increase the adsorption strength of intermediates and increase the rate of methanol synthesis (Behrens, et al., 1996)

$Cu/ZnO/Al_2O_3$ is a commercial catalyst used in industry. It is known that this catalyst has acidic properties which favor the synthesis of dimethyl ether (DME) from syngas which could be derived from coal, biomass and natural gas. The synthesis process devided into two steps. First step is the hydrogenation of CO or CO_2 on Cu-ZnO based catalysts and second step is where DME is produce by the dehydration of methanol on the solid acid catalysts, γ-Al_2O_3 (Ma et al., 2003). Meanwhile Jung et al. (2012) reported that the formation of methanol can be increased by increasing the copper surface area with large amount of acidic sites. The authors also emphasize that the amount of acidic sites are more crucial for high yield of DME from syngas.

2.3.2. Cu/ZnO/ZrO_2 catalyst

Zirconium Oxide (ZrO_2) is a crystalline compound that used specially as thermal and electric insulation. Due to it conductivity, Zr is known as electroceramics and used as fuel cell membranes because its ability to allow oxygen ions to move freely on its crystal structure.

Studies found that ZrO_2 is an interesting compound that can act as support material to Cu-based catalysts and able to enhance the activity for methanol synthesis. The incorporation of ZrO_2 into Cu-based catalysts enhances catalytic performance in steam reforming reaction (Agrell et al., 2003). The authors also mention that, catalysts containing ZrO_2 are more resistant to redox cycles and have high stability.

It is known that Zr act as promoter and improve the dispersion of copper oxide (CuO) on the surface of the catalyst. Interaction of metal Cu particles with both ZnO and ZrO_2 promote the stabilization of $Cu^{\delta+}$ sites at the metal oxides interface and encourage the formation of reactive formate intermediate via CO_2 adsorption (Arena, et al., 2008) and become the rate limiting step of methanol synthesis (Fujitani et al., 1997).

Cu/ZnO/ZrO_2 catalysts are found to show a good activity for methanol synthesis under low temperature and pressure for CO hydrogenation. This is because the presence of ZrO_2 change the surface area of Cu and adjust the ratio of Cu^{+}/Cu° of on the surface of Cu particles to increase the specific activity for CO hydrogenation (Suh et al., 2000).

According to Jones et al. (2010) the impregnation of ZrO_2 on the nanoparticle catalyst increase the methanol reforming reaction and produce low level of CO. At the same time suppress the reverse water gas shift reaction and methanol decomposition.

2.3.3. Catalyst deactivation

Catalyst deactivation refer to the loss of activity and selectivity of a catalyst used in a process. It is important for a catalyst to have longer life span and retain its activity. This is very concern in industrial catalytic processes because catalyst replacement or regeneration is very expensive. Catalyst deactivation is mostly caused by the process design.

Deactivation of catalyst is inevitable and so far there are five major causes of deactivation which are poisoning, fouling, thermal degradation, mechanical damage and corrosion or leaching. Below are the brief description on mechanism of catalyst deactivation (Bartholomew, 2001):

Table 3: Mechanism of catalyst deactivation

Mechanisms	Type	Brief definition/description
Poisoning	Chemical	Strong chemisorptions of species on catalytic sites, thereby blocking sites for catalytic reaction
Fouling	Mechanical	Physical deposition of species from fluid phase onto the catalytic surface and in catalyst pores
Thermal degradation	Thermal	Thermally induced loss of catalytic surface area, support area and active phase-support reactions
Vapor formation	Chemical	Reaction of gas with catalyst phase to produce volatile compound
Vapor-solid and solid-solid reactions	Chemical	Reaction of fluid, support, or promoter with catalytic phase to produce inactive phase
Attrition/crushing	Mechanical	Loss of catalytic material due to abrasion Loss of internal surface area due to mechanical-induced crushing of the catalyst particle

Regeneration of catalyst is possible and often done at the end of the cycle life of the catalyst where the catalyst will be recycled and treated. This is much more economical rather than disposed and buying new catalyst. Cao et al. (2006)

conclude that $ZnO\text{-}Cr_2O_3/CeCO_2\text{-}ZrO_2/Al_2O_3$ (Zr-Cr) catalyst is a promising catalyst for hydrogen production from methanol-steam reforming. They found that the catalyst did not experience significant deactivation over 300 minutes of continuous operation. They noticed that with the absence of water, the catalyst deactivated rapidly due to coke formation and the addtion of water into the feed changed the route of methanol conversion.

Cu-based supported catalysts are principally used in large-scale commercial processes for methanol synthesis. Thus, lifetime of Cu catalysts and deactivation behavior are important to meet optimal process conditions and economic viable. The deactivation of Cu catalysts are mainly due to thermal sintering of metallic Cu particles and it is accelerated when CO-rich feed was used (Sun et al., 1999). Meanwhile Kurz et al., (2003) stated that the activation of Cu crystallites contribute to thermal sintering of the catalyst and Al_2O_3 inhibitng the thermal sintering of Cu crystallites for Cu/ZnO catalysts.

2.4. Catalyst preparation

The effect of catalyst on the activity and selectivity of process has become a major focus in the research and development area. Various study have been conducted to determine the optimum catalyst in high conversion and high selectivity of the determine process. Based on the research, the performance of the catalyst is affected by its preparation method. Few factors are listed in determine the qualities of the catalyst:

- High metal surface area give to higher active metal sites.
- High thermal stability to endure extreme operating temperature.
- High dispersion and homogeneity to prevent the catalyst from agglomerate.
- High mechanical stability to withstand higher pressure.

Even though the performance of the catalyst is affected by the surface area of the active sites, it is also required a stabilizing compound that will increase the tendency of the catalyst from poisoning and fouling. Thus, preparation method of the catalyst is a major aspect in determine the activity and selectivity of the process. There are various

method in preparing the catalyst such as impregnation, precipitation, sol-gel matrices (Obert & Dave, 1999) and combustion synthesis (Guo et al., 2009).

Type of preparation for the catalyst plays an important role because it affect the structure, surface properties and the catalyst precursors. Based on Kimet al., (1998), the catalyst prepared by microemulsion method exhibited higher activity than that prepared by impregnation method and particle size of the catalyst could be controlled by the concentration of metal salts in water pools. Meanwhile Zhang et al., (1997),stated that post treatment for precipitate has a remarkable effect on the structure and catalytic activity for $Cu/ZnO/Al_2O_3$ catalysts for methanol synthesis where washing the precipitate with deionised water leads to larger metallic particle size, cause smaller surface area and weak synergy interaction between copper and ZnO.

One of preparation method that play important role in the catalyst performance is the calcination process. Calcination is a thermal treatment process used to drive off water and remove volatile fraction. It is also purposely used to cause physical or chemical constitution of chemical compound. There are very few study conducted on the effect of calcination towards Cu/Zn catalysts based. According to Al-Zeghayer and Jibril (2005) there are correlation between calcination temperature and the active metal of the catalysts. The author found that increasing the calcination temperature will increase the interaction of active metal with alumina support on y-Al2O3-supported CoMo hydrodesulfurization catalysts. Meanwhile Zhang et al., (2007) stated, it is important to determine the right calcination parameter. If the calcination temperature used is to high, it will cause the catalyst precursor to decompose which decline the surface area of the catalyst and yield of the desired products. As can be seen, the calcination do affect the performance of the catalyst especially on active metal and support of the catalyst especially on the morphology of metal oxide promoter (Yu et al., 2011). Calcination help to improve the interaction of the active metals on the surface of the catalyst support, it help to stabilize the catalyst and prevent them from undergo sintering process (Centeno et al., 2003).

2.5.1. Deposition precipitation preparation method

Deposition precipitation is the precipitation process of a metal precursor onto a suspended support material .Meanwhile co-precipitation is the mixing of two or more active salts and undergo neutralization process and form multi complexes bond.

In catalyst preparation, the nature of the support is very important because it affect the dispersion of the active sites of catalysts as mentioned by Centeno et al., (2002). Furthemore optimal experiment conditions required to obtain homogeneous distribution on the catalyst surface especially the acid-base properties of the support that encourage selective deposition on the oxides particles (Centeno et al., 2003).

For this project, deposition precipitation will be used by depositing the metal salts on the surface of carbon nanofiber because it influence the surface of the catalyst and produce finer particles which result higher catalytic if compare to the catalyst prepared by impregnation and co-precipitation (Raudaskoski et al., 2009).

2.5. Catalyst characterization

For this project we will focus on carbon nanofiber supported Cu/ZrO_2 catalyst which will be used for CO_2 hydrogenation. The catalyst will be produced by using deposition co-precipitation method. The catalyst will undergo several characterization test as it is important to compare the result with current studies.

2.5.1. Thermal gravimetric Analysis (TGA)

Thermal gravimetric analysis (TGA) is known as a method that used to determine the thermal stability of component and its fraction of volatile components within it by monitoring the changes in weight as the specimen is heated.

The type of specimen will determine the possible heating program and for this project the analysis is conducted in inert atmosphere. To prevent the oxidation of the catalyst. The sample is heated at constant heating rate and throughout the heating, the changes in weight will be recorded.

The results will be displayed as mass against the temperature of time as to analyze changes in mass at every given temperature. TGA is a useful method to study the physical properties of the tested specimen such as vaporization, sublimation, adsorption, desorption and absorption (Brown, 2001).

2.5.2. X-ray diffraction (XRD)

X-ray diffraction (XRD) is a method that used in determine the structure of the solid. Solid can be classified into two categories, crystalline structure and amorphous solids. In solids, atoms are arranged in a regular pattern and by repetition this form the crystal structure. X-ray will be emitted and pass through the crystalline materials, then the diffracted rays will determine the structure .

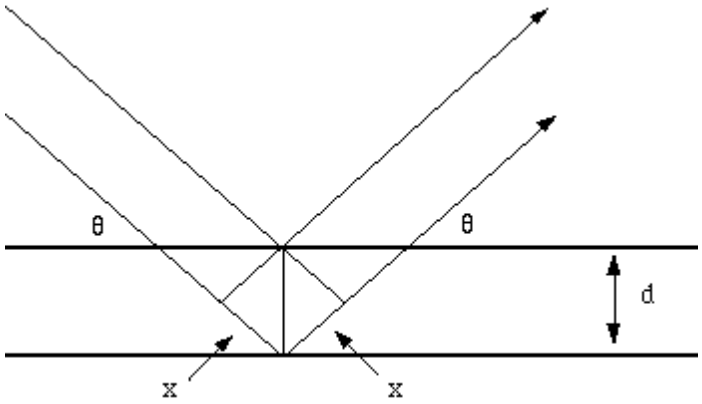

Figure 3: X-ray reflection on two atomic planes of crystalline solid

The scattered radiation will be observed only in directions where the beams are reflected from crystal plane which amplified by interference. The two parallel incident rays (1) and (2) will form an angle, Θ. A reflected beam of maximum intensity will result if the waves (1) and (2) are in phase. The difference in path length between (1) to A and (2) to B will be labeled as *d* which determine the integral number of wavelengths, *λ*. *n* is an integer. This can be express mathematically in Bragg's law:

$$n\lambda=2d \sin \Theta$$

2.5.3. Temperature programmed reduction (TPR)

Temperature Programmed Reduction is commonly used to identify the reduction condition of the catalyst. It give quantitative measurement of the catalyst changes under thermal conditions with the presence of reductive gases. The reductive agent used usually a mixture of 5% hydrogen in an inert gas .

This analytical method widely used because it give great information on the studied sample. Listed below are the information that can be obtained:

- Optimum reduction temperature
- Amount of active sites present in the catalyst
- Dispersion of active metals on the catalyst surface
- Active metal particle size in catalyst

2.5.4. BET analysis

BET analysis or Brunauer-Emmet-Teller (BET theory) is an analytical method that use extension of Langmuir theory to determine the surface area of particle through the physical adsorption of inert gas on the surfaces. BET surface area measurement is crucial in understanding the behavior of material. Materials do react with its surroundings via its surface. Furthermore, the kinetic reaction of a material depend on its surface area. Typical analysis that can be found by using BET analysis :

- Specific surface area
- Pore size analysis
- Micropore analysis
- Pore size distribution
- Percentage of porosity

CHAPTER 3: METHODOLOGY

3.1. Materials and Apparatus

Table 4: List of chemicals used

Chemical	Supplier	Purity (%)	Usage
Urea	Acros	99.5	Precipitating agent
Carbon-Nanofiber	Carbon Nano-Material Technology Co., Ltd, Korea	-	Catalyst support
Copper (II) Nitrate Trihydrate	MERCK	99.5%	Catalyst precursor
Zirconia Nitrate Hexahydrate	Acros	99.5%	Catalyst precursor

Table 5: Equipment used in the experiment

Equipment	Capacity	Quantity
Beaker	1000ml	1
Beaker	500ml	1
Conical flask	1500ml	1
Cylinder	500ml	1
Cylinder	100ml	1
Porcelain	-	6
Pipette/Burette	250ml	1
Magnetic stirrer	-	2
Oven	-	1
Furnace	-	1
Membrane filter	-	6
pH meter	-	1
Thermometer	-	2
Conical filter	-	2
Syringe	10ml	6

3.2. Activation of Carbon Nanofiber (CNF)

Prior to metal loading, carbon nanofibers (CNFs) with purity of 99%, length 20-200 μm and diameter of 10 nm purchased from Carbon Nano-material Technology Co. Ltd, Korea, were functionalized and activated. In this process, 10 grams of CNFs were treated with 65 vol% of nitric acid (HNO_3) for 2 hours at 70˚C. The mixture was then cooled to room temperature and diluted with 1500 mL of deionized (DI) water.

The mixture was filtered using Buchner funnel to separate the activated CNFs from the solution. The activated CNFs were dispersed in 500 mL of DI water and left stirred overnight. Subsequently the solution was filtered and the activated CNFs were rinsed with DI water until the pH of the filtrate was neutral. The sample was left to dry overnight at 110˚C.

3.3. Deposition of CNF catalyst support-Cu/ZrO_2

In this project, Cu/ZrO_2 catalyst and CNF as its support with fixed composition will be used (20% Cu and 5% Zr). The catalyst was prepared by deposition precipitation method. Cu was obtain from copper nitrate trihydrate [$Cu(NO_3)_2.3H_2O$] and Zr from zirconia nitrate hexahydrate [$Zr(NO_3)_4.6H_2O$]. Meanwhile urea (CH_4N_2O) act as precipitating agent.

The catalyst was prepared by using 1 gram of activated CNF as the weight basis. The components were mixed together and added with DI water to dissolve the mixture. The solution was heated up and maintain to 90˚C. Urea solution with 2.7 M was added dropwise into the solution for deposition precipitation to take place on the surface of the CNF.

The slurry was left under vigorous stirring for 18 hours. After precipitation, the suspension was filtered and washed with DI water for several times. The precipitate was dried overnight at 120˚C. After drying, the catalyst was calcined in the furnace. The procedure was repeated to prepare catalyst at different calcination temperature (250˚C, 350˚C, 450˚C and 550˚C) and duration (3hours, 4hours and 5hours).

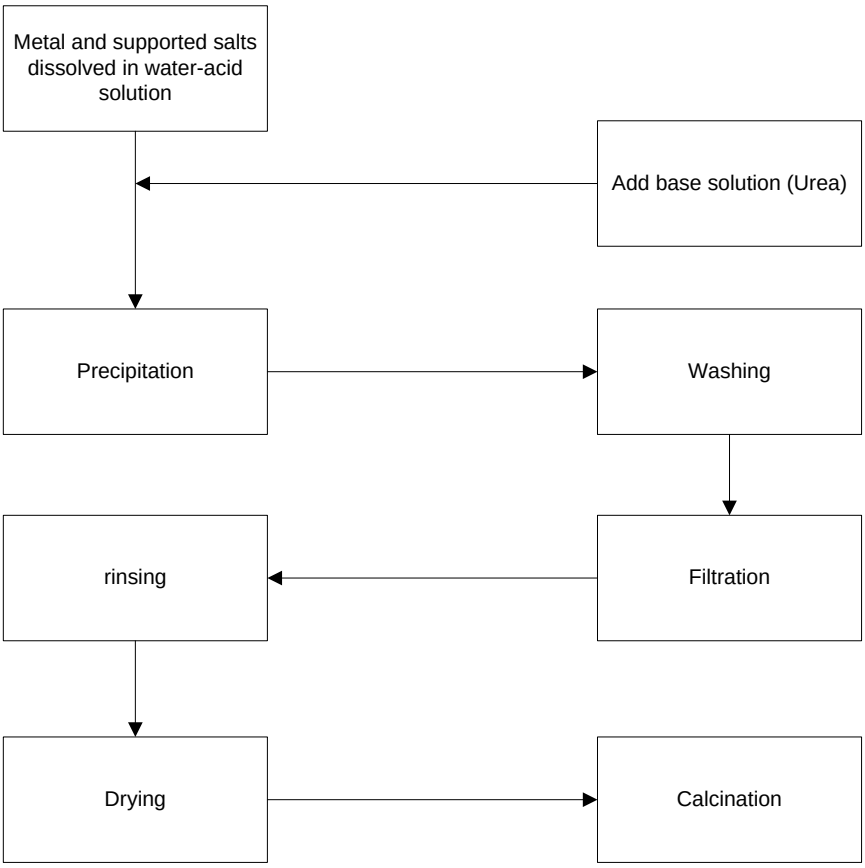

Figure 4: Deposition precipitation flow process

Table 6: Samples prepared

Sample ID	Calcination Temperature (˚C)	Duration (Hours)
CCZ 1	250	4
CCZ 2	350	4
CCZ 3	450	4
CCZ 4	550	4
CCZ 5	550	3
CCZ 6	550	5

3.4. Catalyst characterization

Before proceed with reaction studies, the prepared catalyst will be tested for characterization using the following method: Thermal Gravimetric Analysis, X-ray diffraction, Temperature Programmed Reduction and BET analysis.

3.4.1. Thermal Gravimetric Analysis (TGA)

The prepared catalyst was tested with TGA to determine weight changes with increasing temperature. 0.30 gram of the catalyst is analyze using Perkin Elmer Thermo gravimetric equipment. The sample was heated under a flow of inert gas which to prevent the sample from oxidize . Nitrogen gas was used in this analysis with a flow rate of 20 ml/min and at a constant heating rate of 10˚C/min.

The heating started from room temperature to 800˚C and the weight of the catalyst was recorded at each 10˚C interval until the heating process ended. The changes in weight of the catalyst against the increasing temperature was plotted to determine the thermal stability of the sample.

Figure 5: Thermal Gravimetric Analyzer Perkin Elmer Pyris 1

3.4.2. X-ray diffraction (XRD)

After the calcination of the catalyst, the samples were tested to determine the crystalline structure by using XRD method. 0.30 gram of the calcined catalyst was analyze with Diffraction Bruker-AXS D8 Advance and use monochromatize Cu/Kα was used as the radiation source. The crystalline structure present in the catalyst was identified by comparing the scanning angles and d-spacing of each peak that produced from the diffracted radiation.

XRD analysis was repeated for each sample of the catalyst prepared at different calcination parameters. This is to investigate the relationship of calcination parameters on the crystal structure of the catalyst.

Figure 6: X-Ray Diffraction Bruker-AXS D8 Advance

3.4.3. BET analysis

BET analysis is a method used to determine the surface area of the catalyst, pore volume and the average pore size of the sample. Micromeritics ASAP 2020 is the equipment that will be used to conduct the analysis. 0.30 gram of the calcined catalyst was degased with nitrogen gas before proceed with BET analysis.

The sample was degas at constant heating rate of 10˚C/min up to 90˚C for 30 minutes to prevent the sample from thermal shock and then proceed to 300˚C for 240 minutes. The degas process is to remove remaining volatile particles before surface area and pores analysis take place.

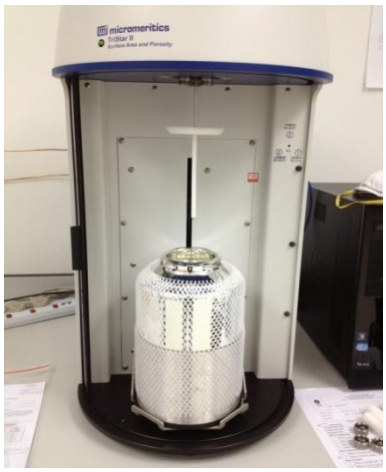

Figure 7: Micomeritics ASAP 2020

3.4.4. Temperature Programmed Reduction (TPR)

TPR is a method to analyze the surface reducibility and optimum reduction temperature of a catalyst species. Hydrogen gas (H_2) act as a reducing agent and undergo adsorption process on the surface of the active metal of the catalyst. It can be considered as qualitative analysis of reduction conditions on the surface of the catalyst.

Thermo Finnigan TPDRO 1100 is the equipment used to perform TPR analysis. This analysis was performed with 5% H_2 gas in an inert argon gas. The

sample is heated from room temperature to 350˚C with ramp rate of 10˚C/min in a flowing gas of H_2 in Ar at 20ml/min for 2 hours. As the process take place, the concentration of the hydrogen in gas mixture decreasesed as the catalyst adsorb H_2 gas on its surface. This changes was detected by thermal conductivity detector (TCD) and interpreted into graphical plot. From the graph, the highest peak will be identified as the optimum reduction temperature.

Figure 8: TPDRO 1100 Series

3.5. Catalytic Activity

3.5.1. Catalyst Activity Study

In this project, stirred reactor Parr 4590 was used to study the CO_2 hydrogenation reaction. The reactor was preheated before the reaction started. The reactions were conducted in liquid phase. Operating condition in the reactor was set to 30 MPa and 443 K (170 ˚C). Initially, 0.5 gram of the prepared catalyst was mixed together with 25 mL of ethanol.

The catalyst was activated by reduce it in H_2 gas at reduced temperature 350˚C based on TPR analysis. A pressurized mixture of H_2 and CO_2 with ratio of 3:1was introduced into the reactor. Once the desired operating conditions achieved, the reaction was allowed to take place for 3 hours under vigorous

stirring. At the end of the reaction, gas and liquid samples were collected to determine the conversion, selectivity and yield of the reaction.

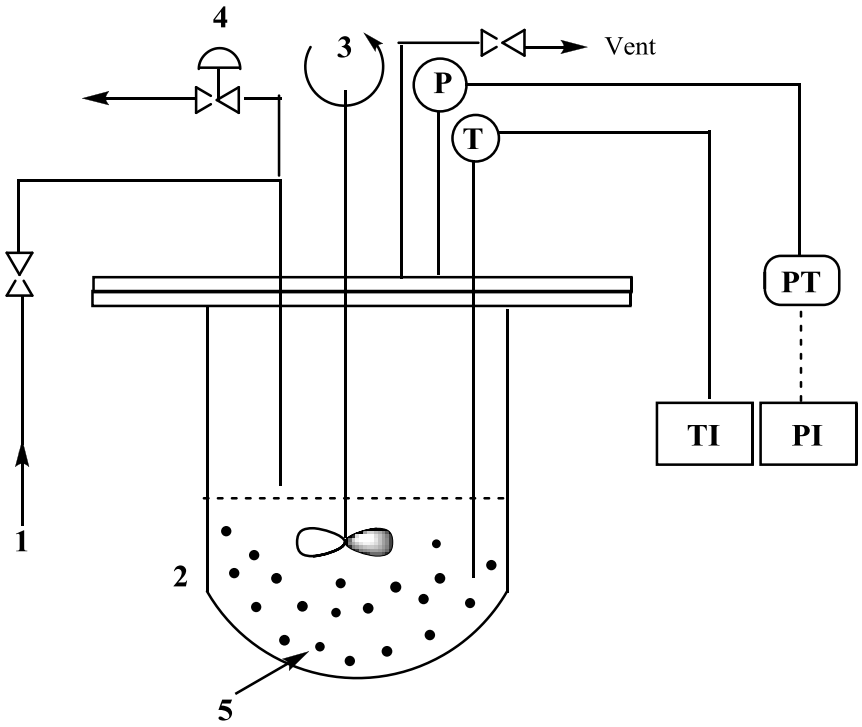

Figure 9: Schematic of the experimental setup: (1) premixed CO_2/H_2; (2) high pressure reactor; (3) stirrer; (4) sampling valve; (5) powdered catalyst; (T) thermocouple; (P) pressure gauge; (PT) pressure transducer; (PI) pressure indicator; (TI) temperature indicator

3.5.2. Analytical Technique

Gas Chromatography is an analytical method widely used in laboratory to determine the organic compounds present in the mixture. The concept of chromatography is to separate and analyze compounds through vaporization. Gas chromatography able to separate sample and determine the amount of component present. This was done by the aid of injection port where sample are loaded, a column which components are separated, carrier gas that carries the sample, a detector and data processor. There are two methods to be used in this work; gas phase analysis and liquid phase analysis.

3.5.2.1. Gas Phase Analysis

Gas phase analysis was used to analyze the gas mixtures. For this work the gases to be analyzed are H_2 and CO_2 gas. For this analytical technique, a dedicated detector was used which is Thermal Conductivity Detector (TCD) to determine the amount of the components present. The analysis is conducted based on the comparison of two gas streams, carrier gas and compound gas. The gas is passed over a heated filament wire, the difference of the resistance due to the thermal conductivity of the gas will be registered on the recorder and used to determine the concentration of the sample component. Normally, helium and hydrogen are used as carrier gas due to its high thermal conductivity and cause the largest resistance difference in the presence of sample component gases.

Table 7: Operating conditions for TCD GC

Temperature (˚C)	200
Pressure (kPa)	55.9
Carrier gas	Helium
Column holding temperature (˚C)	35˚C
Ramp time	40˚C/min
Column type	GC-Q 113-3422
Column length (m)	25
Column ID (mm)	0.32
Column flow (ml/min)	0.99
Linear velocity (cm/sec)	19.8

Figure 10: Shimadzu GC-17A used for gas phase analysis

3.5.2.2. Liquid Phase Analysis

Methanol and ethanol content were analyzed using liquid phase analysis. For this analytical technique , Flame Ionization Detector (FID) was used. FID is a very sensitive and able to detect all organic substances especially hydrocarbons. It is also mass sensitive and require a very stable gas flow. The response of FID depends on the number of carbon atoms in the sample and the oxidation state of carbon. This method use pyrolysis technique to analyze the sample. Several gases are used to operate FID gas chromatography which are hydrogen, oxygen and carrier gas. Below are the operating conditions for FID;

Table 8: Operating conditions for FID GC

Injection temperature (˚C)	250
Detector temperature (˚C)	260
Pressure (kPa)	77
Ramp time (˚C/min)	50˚C/min
Carrier gas	Helium
Column type	BP-20 SGE
Column length (m)	30
Column ID (mm)	0.25

Column temperature (˚C)	50
Column flow (ml/min)	1.00
Linear velocity (cm/sec)	26.1

Figure 11: Shimadzu GC-2010 used for liquid phase analysis

3.5.2.3. Karl Fischer Titration

Karl Fischer Titration is an analytical method used to measure water content in a given sample. It was founded by a German Chemist named Karl Fischer in 1935. The working medium of Karl Fischer titration is utilizing the quantitative reaction of water with iodine reagent and the amount of the water content determine by using stoichiometry of Karl Fischer reaction. There are two type of Karl Fischer method, coulometric titration and volumetric titration. Coulometric titration is used to detect low concentration of water meanwhile volumetric titration is used to determine unlimited range of water content. Coulometric titration require two reagents which are iodide and sulphur dioxide act as an anolyte. Water react with reagents by electrolysis reaction and the water content is determine by the amount of electricity produced. For this work, volumetric titration is used to analyze water content of the sample. The reagents are used as titrant solution to dissolve water in the sample. The amount of reagents consumed will determine the amount of water

present in the sample. Mettler Toledo V30 Volumetric KF Titrator was used and the reagents used are CombiTitrant 5 Keto and CombiSolvent Keto.

Figure 12: V30 Volumetric KF titrator

3.6. Key Milestones

Below are the key milestones that have been determine for this project to be completed in proposed timeline and at the same time achieved the stated objectives:

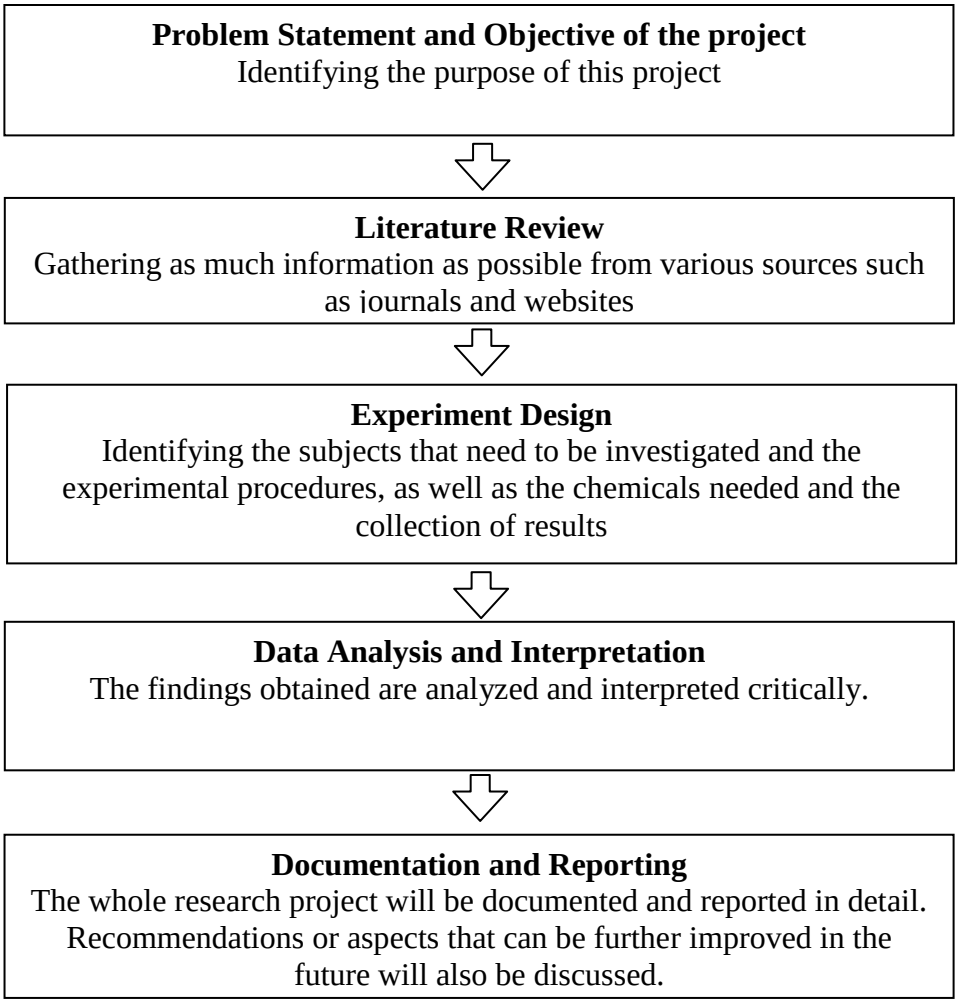

3.7. Gantt Chart

Table 9: FYP II Gantt Chart

No.	Detail/Week	1	2	3	4	5	6	7		8	9	10	11	12	13	14	15
1	Project Work Continues																
2	Submission of Progress Report																
3	Project Work Continues																
4	Pre-EDX																
5	Submission of Draft Report																
6	Submission of Dissertation (Soft Bound)																
7	Submission of Technical Paper																
8	Oral Presentation																
9	Submission of Project Dissertation (Hard Bound)																

Process
Mid Semester Break
Suggested Milestone

CHAPTER 4: RESULT AND DISCUSSION

4.1. Thermal Gravimetric Analysis (TGA)

TGA is one of method used to determine the calcination temperature of the catalyst. The mass change of the substance as a function of temperature or time was analyzed when the specimen was heated. A fresh uncalcined was tested.

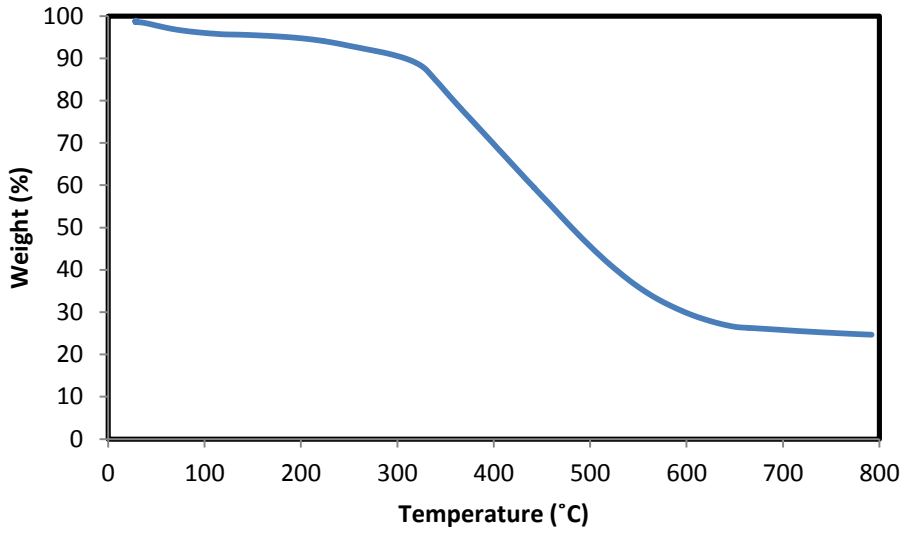

Figure 13: TGA profile for CCZ catalyst

As can be seen from the graph, the catalyst having a slow degradation at 30˚C to 300 ˚C. But at 350˚C, the catalyst started to degrade aggressively and stop between 600˚C and 700˚C.

At temperature ranging from 30˚C to 300˚C, the loss of mass is mainly caused by the loss of water in the catalyst. Referring to the boiling temperature for copper nitrates (170˚C) and zirconium nitrate (100˚C) at atmospheric temperature. It can be indicates that within that temperature range, the unreacted nitrates are also oxidized.

From the graph at temperature ranging from 350˚C to 600˚C, the catalyst decomposed tremendously. It is believe that in this range, the CNF which was not deposited by Cu and ZrO_2 was decomposed According to Balan et al. (2010), the metal nanoparticle dispersed on CNF surfaces can act as active sites that facilitate the oxidation of carbon which lead to fast decomposition at lower temperature compared to CNF sample.

4.2. X-Ray Diffraction

X-Ray Diffraction is used to study the structure and morphology of the CCZ catalyst that being calcine at different temperature. The catalyst was scanned with X-ray at different range 2-80˚ and the type of crystallite present in the sample was identified by comparing the scanning angle and d-spacing of each peak with the ones in material library.

Calcination is one of crucial step in preparing the catalyst. This is because in this step, unwanted salts are properly remove and at the same time encourage oxidation on the catalyst surface. For this study, the samples were calcine at different temperature (250˚C, 350˚C, 450˚C, 550˚C) and duration (3 hours, 4hours, 5 hours) to determine the optimum parameters of the catalyst. After the calcination process, the samples are analyzed to determine the metal phases present in the catalyst.

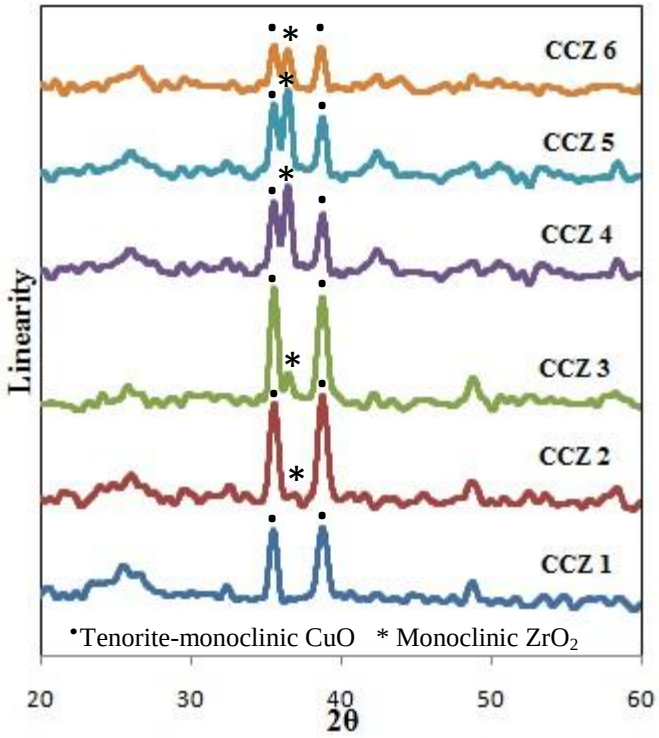

Figure 14: XRD patterns of CCZ catalysts calcined at different temperature duration

The XRD patterns that characterized the structure of the catalysts synthesized are shown in Figure 14. The poor crystallinity of CCZ catalyst is shown by the low signal-noise ratio. Only a few peaks can be seen above the baseline. Two ell-defined peaks visible at 2θ= 35.5˚ and 38.9˚ were ascribed to a typical structure of the tenorite, a monoclinic structure of CuO with crystal plane (1̄11) and (200) (Guo et al., 2011). Thus, it can be deduced that the copper species in the precursors calcined at 250˚C have been converted to CuO. With the increase in calcination temperature, the diffraction peaks of CuO and monoclinic zirconia (m-ZrO_2) become stronger and sharper simultaneously which indicate a continuous increase in crystallization degree of CuO and m-ZrO_2. According to the XRD analysis, the copper oxide (CuO) occurs at Bragg's angle of 35.4˚ and 38.7˚. For zirconium oxide (ZrO_2) the peak is present at 36.4˚.

It is suggested that the calcination should not be conducted at temperature below 550˚C because this does not promote or oxidize Zr metal in the catalyst which act as the catalyst promoter and hence reduce the performance of the catalyst. Long duration of

calcination actually reduce the metal phase of the catalyst as can be seen on the graph where the peak intensity is reduced at duration more than 4 hours.

Table 10: Metal phase present in the catalyst

Catalyst Series	Sample	Copper Oxide	Zirconium Oxide
CCZ	CCZ 1	Tenorite-monoclinic	-
	CCZ 2	Tenorite-monoclinic	-
	CCZ 3	Tenorite-monoclinic	Monoclinic
	CCZ 4	Tenorite-monoclinic	Monoclinic
	CCZ 5	Tenorite-monoclinic	Monoclinic
	CCZ 6	Tenorite-monoclinic	Monoclinic

4.3. Temperature Programmed Reduction (TPR)

TPR commonly used as to analyze the surface reducibility of the catalyst and optimum reduction temperature for the catalyst. The data from TPR analysis for each sample is collected and a graph of amount of H_2 gas adsorbed vs temperature was plotted and shown in Figure 15.

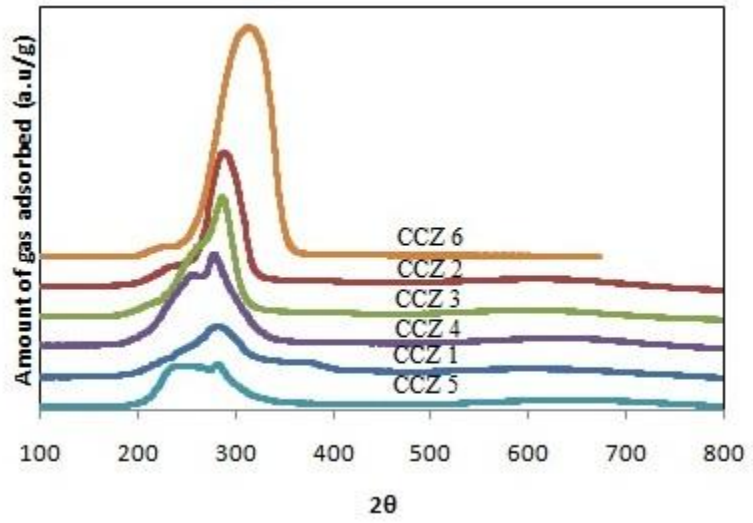

Figure 15: H_2-TPR profiles of the CCZ catalysts

It can be seen that CCZ 5, CCZ 1, CCZ 4 and CCZ 3 exhibit a broad band of H_2 consumption in the range of 220-330˚C. The slope of this band of H_2 consumption, which is asymmetric with a shoulder or a tail, is the result of a complex overlapping of several elevated reduction process (Bae et al, 2009). Since ZrO_2 is not reduced within the experimental regions (GuO et al., 2011), the reduction peaks are related to the reduction of CuO species. With the calcination temperature and duration increasing, the peak shift to higher temperature accompanied by an increase in the narrowness of the peak. This indicates the particle sizes of CuO increase form 250-550˚C because the higher the reduction temperature is, the larger the CuO particle will be.

4.4. BET Analysis

The result of BET surface area analysis is presented in the table below. The analysis is conducted for each CCZ that have been calcine at different temperature to determine the surface area, pore size and pore volume of the catalyst using Micromeritics ASAP 2020.

Table 11: BET result

Sample	BET Surface Area(m^2/g)	Pore Size (Å)	Pore Volume (cm^3/g)
CCZ 1	111.30	71.27	0.20
CCZ 2	69.05	76.99	0.13
CCZ 3	27.13	138.02	0.10
CCZ 4	11.87	165.81	0.05
CCZ 5	140.11	55.05	0.19
CCZ 6	19.67	120.15	0.06

It can be seen from Table 11, calcination temperature affect the structural properties of the catalyst. The BET surface area decreased from 111.30m^2/g of CCZ 1 to 11.87 m^2/g of CCZ 4 and the variation trend is consistent with the result of XRD. The growth

of crystal grain and/or the agglomeration of particle with the increase in calcination temperature are responsible for the change of the surface area.

The trending is obvious that as the temperature and duration used in the calcination process increases, the surface area and pore volume decrease but at the same time the size of the pore increases. It is been reported that the change in surface area of the catalyst could alter the surface area of the copper. Thus, affecting the catalytic activity of the catalyst in methanol synthesis (Bae et al., 2009). Study found that larger pore size also encourage the catalytic activity of the catalyst because with large pore diameter, the mass-transfer effects of reactants and products are easily takes place (Jung et al., 2012).

4.5. Analytical Results

Catalyst activity was studied using a stirred reactor. A pressurized mixture of H_2 and CO_2 with ratio of 3:1 was introduced into the reactor under vigorous stirring. Two analyses are conducted, gas phase analysis and liquid phase analysis used to analyze the composition of the reaction products. The analytical studies is conducted using gas chromatograph.

4.5.1. Liquid phase analysis

There are altogether six samples to be analyzef by Flame Ionization Detector (FID) gas chromatography. For liquid phase analysis, component to be analyze is methanol that present after the reaction take place. Below are the equation used to determine the methanol yield from the reaction:

$$\text{Methanol yield (\%)} = \frac{Mole\ of\ methanol\ produced}{Mole\ of\ CO_2 feed} \times 100 \qquad (1)$$

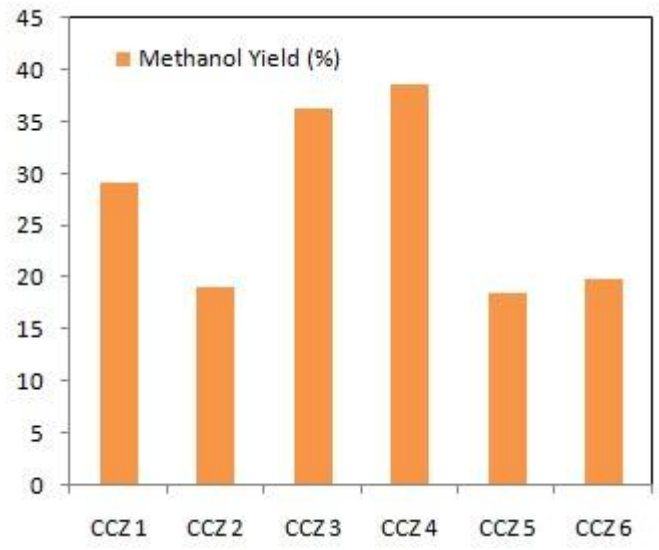

Figure 16: Methanol yield (%) for each sample

From the result obtained, it shows that CCZ 4 has the highest methanol yield, 38.67 %. This can be explained because it has the highest metal surface which favor higher catalytic activity compare to the others based on TPR profiles. Furthermore, CCZ 4 has more defined Zr metal phase and bigger pore size which allow more methanol to be synthesized.

4.5.2. Gas Phase Analysis

Gas sample collected at the end of the reaction will be analyze using Thermo Couple Detector (TCD) gas chromatography. The gas to be analyze is CO_2 as to determine the percentage of CO_2 conversion rate . The formula used to determine the percentage of CO_2 conversion rate is as below:

$$X_{CO_2}(\%) = \frac{n(CO_2)_0 - n(CO_2)_t}{n(CO_2)_0} \times 100 \quad (2)$$

where:

$n(CO_2)_o$ is the mole fraction of CO_2 in feed gas sample.

$n(CO_2)_t$ is the mole fraction of CO_2 in product sample.

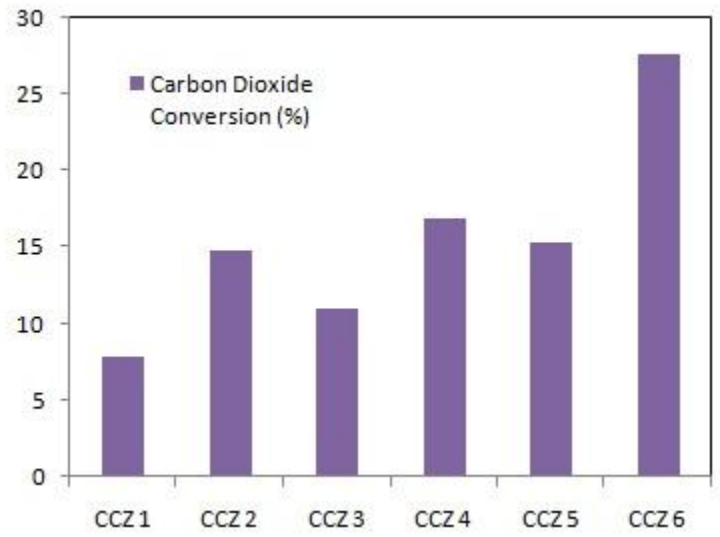

Figure 17: Carbon Dioxide conversion (%) for each sample

From the graph plotted, the carbon dioxide conversion increase with the increase of the calcination temperature and duration used on the catalyst. According to the BET analysis, higher temperature of the calcination used will increase the pore size of the catalyst. As the size of the pore increase, more carbon dioxide can be adsorb on the surface of the catalyst and favor the conversion of CO_2 the methanol. Based on the result, CCZ 6 has the highest carbon dioxide conversion compare to the others.

4.5.3. Water Content Analysis

The product collected at the end of the reaction was analyzed using V30 Volumetric KF Titrator to determine the amount of water produced during the methanol synthesis. Below are the data collected on the amount of water produced from reverse water-gas shift reaction:

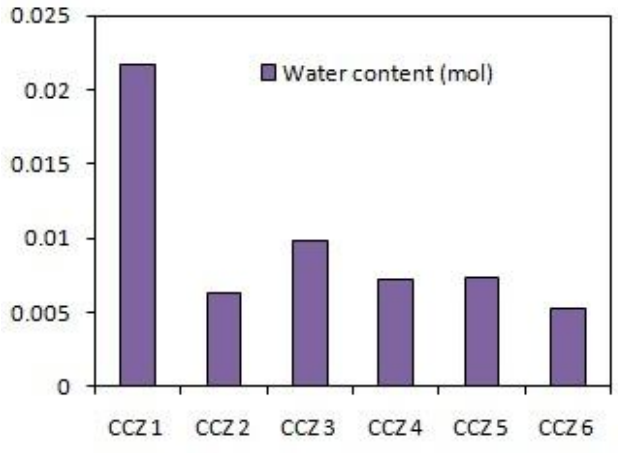

Figure 18: Water content in mass percent (%)

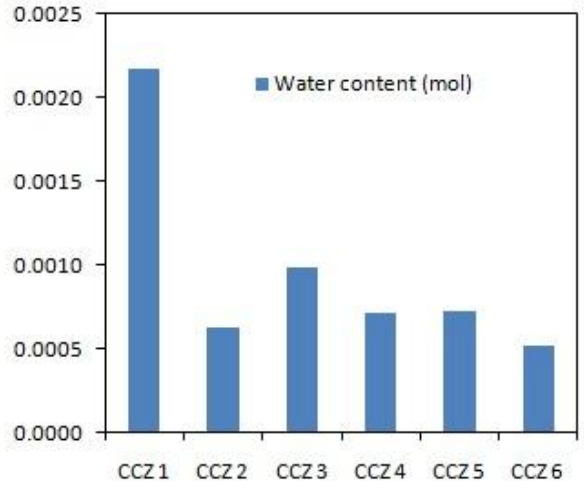

Figure 19: Water content in mol

The selectivity of methanol in this reaction is calculated using the following equation:

$$S\ (\%) = \frac{P_i}{\sum P_x} \quad (3)$$

where:

P_i is the mole of methanol in product sample.

$\sum P_x$ is the total mole of components in product sample.

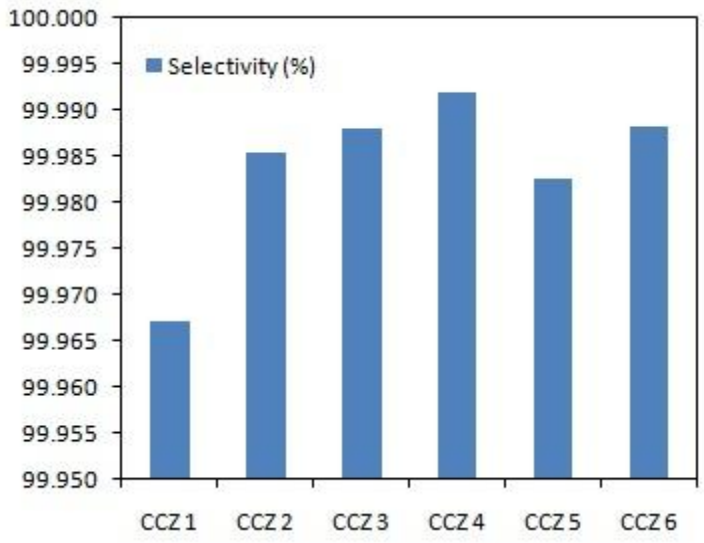

Figure 20: Selectivity of methanol (%)

From the graph plotted CCZ 6 has the lowest amount of water produced from reverse water-gas shift reaction and CCZ 5 has the highest selectivity of methanol (99.99%) compare to the other samples. However, calcination temperature and duration do not have significant effect on the selectivity of the CO_2 hydrogenation to methanol.

CHAPTER 5: CONCLUSION AND RECOMENDATION

From the studies conducted , the calcination parameters to be studied (temperature and duration) affect the structural properties and the activity of the catalyst. With the increase in calcination temperature, the intensity of m-ZrO_2 peak increased when the calcination temperature is above 250˚C. As the temperature of the calcination increase, the metal peak intensities of CCZ catalyst also increased and more defined. Beside that it also affect the size of the pores and the metal surface of the catalyst. Low calcination temperature used favor high surface area and pore volume of the CCZ catalyst but higher calcination temperature promotes greater pore size of the catalyst. Meanwhile changes in calcination parameters do not affect the reduction temperature of CCZ catalyst but it affect the area under the reduction peak which explain the homogeneity dispersion of the active metal.

From the activity studies conducted in a stirred reactor Parr 4590 with H_2 and CO_2 ratio 3:1 at 3.0MPa and 443 K (170˚C) , optimum calcination parameters for CCZ catalyst is 550˚C and 4 hours as it produce highest methanol yield and selectivity. It can be concluded that, it is important to determine the optimum calcination of the catalyst as it affect the performance of the catalyst and reaction outcome.

It is recommended to perform kinetic studies on the CCZ catalyst as to further understand the nature of the catalyst and perform TGA of the activated CNF in order to compare the thermal stability before and after deposition of active metal.

REFERENCES

Agrell, J., Birgersson, H., Boutonnet, M., Melian-Cabrera, I., Navarro, R., & Fierro, a. J. (2003). Production of hydrogen from methanol over Cu/ZnO catalysts promoted by ZrO2 and Al2O3. *Journal of Catalysis 219* , 389-403.

Al-Zeghayer, Y., & Jibril, B. (2005). On the effects of calcination conditions on the surface and catalytic properties of y-Al2O3-supported CoMo hydrodesulfurization catalysts. *Applied Catalysis A: General 292* , 287-294.

Arena, F., Italiano, G., Barbera, K., Bordiga, S., Bonura, G., Spadaro, L., et al. (2008). Solid-state interactions, adsorption sites and functionality of Cu-ZnO/ZrO2 catalysts in the CO2 hydrogenation to CH3OH. *Applied Catalysis A: General (350)* , 16-23.

Bae, J. W., Kang, S.-H., Murali, G., & Jun, K.-W. (2009). Effect of Al2O3 content on the adsorptive properties of Cu/ZnO/Al2O3 for removal of odorant sulfur compounds. *International Journal of Hydrogen Energy 34* , 8733-8740.

Balan, B. K., Kale, V. S., Aher, P. P., Shelke, M. V., Pillai, V. K., & Kurungot, a. S. (2010). High aspect ratio nanoscale multifunctional materials derived from hollow carbon nanofiber by polymer insertion and metal decoration. *Chemical Communications 46* , 5590-5592.

Bartholomew, C. H. (2001). Mechanisms of catalyst deactivation. *Applied Catalysis A: General 212* , 17-60.

Behrens, M., Studt, F., Kasatkin, I., S. Kuhl, M. H., Pedersen, F. A., Zander, S., et al. (2012). Methanol Synthesis over Cu/ZnO/Al2O3: The Active Site in Industrial Catalysis. *Science 336* , 893.

Brown, M. (2001). *Introduction to Thermal Analysis.* London: Kluwer Academic Publisher.

Burcham, M. M., Herman, R. G., & Klier, K. (1998). Higher Alcohol Synthesis over Double Bed Cs-Cu/ZnO/Cr2O3 Catalyst: Optimizing the yields of 2-Methyl-1-propanol (Isobutanol). *Ind. Eng. Chem. Res.* , 4657-4668.

C.D. Keeling, a. T. (1997). Possible forcing of global temperature by oceanic tides. *Proceeding National Academy of Science 94* , 8321-8328.

Cao, W., Chen, G., Li, S., & Yuan, Q. (2006). Methanol-steam reforming over a ZnO-Cr2O3/CeO2-ZrO2/Al2O3 catalyst. *Chemical Engineering Journal 119* , 93-98.

Centeno, M. A., Carrizosa, I., & Odriozola, J. A. (2003). Deposition-precipitation method to obtain supported gold catalysts: dependence of the acid-base properties of the support exemplified in the system TiO2-TiOxNy-TiN. *Applied Catalysis A: General 246* , 365-372.

Centeno, M., Paulis, M., Montes, M., & Odriozola, J. (2002). Catalytic combustion of volatile organic compounds on Au/CeO2/Al2O3 and Au/Al2O3. *Applied Catalysis A: General 234* , 65-78.

Chinchen, G., Spencer, M., & Whan, K. W. (1987). Promotion of methanol synthesis and the water-gas shift reactions by adsorbed oxygen on supported copper catalysts. *Journal of the Chemical Society, Faraday Transactions 1 : Physical Chemistry in Condensed Phases* , 2193-2212.

Erno, P. (1995). A practical guide to instrumental analysis.

Fujitani, T., Nakamura, I., Uchijima, T., & Nakamura, J. (1997). The knietic and mechanism of methanol synthesis by hydrogentaion of CO2 over a Zn-deposited Cu(111) surface. *Surface Science 383* , 285-298.

Guo, X., Mao, D., Lu, G., Wang, S., & Wu, G. (2011). CO2 hydrogenation to methanol over Cu/ZnO/ZrO2 catalysts prepared via a route to solid-state reaction. *Catalysis Communications 12* , 1095-1098.

Guo, X., Mao, D., Wang, S., Wu, G., & Lu, G. (2009). Combustion synthesis of CuO-ZnO-ZrO2 catalysts for the hydrogenation of carbon dioxide to methanol. *Catalysis Communications 10* , 1661-1664.

http://www.methanol.org/Methanol-Basics/Methanol-Applications.aspx. (2011). Retrieved from http://www.methanol.org/.

Jian-Ping Shen, C. S. (2002). Influence of preparation method on performance of Cu/Zn-based catalyst for low-temperature steam reforming and oxidative steam reforming of methanol for H2 production for fuel cells. *Catalysis Today 77* , 89-98.

Jones, S. D., Neal, L. M., Everett, M. L., & Gar B. Hoflund, H. E.-W. (2010). Characterization of ZrO2-promoted Cu/ZnO/nano-Al2O3 methanol steam reforming catalysts. *Applied surface science 256* , 7345-7353.

Jung, J., Lee, Y., Um, S., & P.J. Yoo, D. L. (2012). Effect of copper surface area and acidic sites to intrinsic catalytic acticity for dimethyl ether synthesis from biomass-derived syngas. *Applied Catalysis B: Environmental 126* , 1-8.

Kim, W.-Y., Hayashi, H., Kishida, M., Nagata, H., & Wakabayashi, K. (1998). Methanol synthesis from syngas over supported palladium catalysts prepared using water-in-oil microemulsion. *Applied Catalysis A: General 169* , 157-164.

Kurz, M., Wilmer, H., Genger, T., Hinrichsen, O., & Muhler, a. M. (2003). Deactivation of supported copper catalysts for methanol synthesis. *Catalysis Letters 86* , 77-80.

Leiviska, O. M. (December 2008). *Modelling in methanol synthesis.* Oulu: University of Oulu.

Liu, J., Shi, J., He, D., Zhang, Q., Wu, X., Liang, Y., et al. (2001). Surface active structure of ultra-fine Cu/ZrO2 catalysts used for the CO2+H2 to methanol reaction. *Applied Catalysis A: General, 218* , 113-119.

M.J Rhodes., A. B. (2005). The effects of zirconia morphology on methanol sythesis from CO and H2 over Cu/ZrO2 catalyst. *Journal of Catalysis 233* , 198-209.

Ma, L., Trans, T., & Wainwright, M. (2003). 22. *Topic in Catalysis* , 295-304.

Moulijn, J., Diepen, A. v., & Kapteijn, F. (2001). Catalyst deactivation: is it predicatable? What to do? *Applied Catalysis A: General 212* , 3-16.

Noor Azeerah, A., Haliza, A. A., & Zulina, A. M. (June 2012). Co-precipitation technology for preparation of solid catalyst in oleochemical processes.

Obert, R., & Dave, B. C. (1999). Enzymatic conversion of carbon dioxide to methanol: Enhanced methanol production in silica Sol-Gel matrices. *Journal American Chemical Society 121* , 12192-12193.

Raudaskoski, R., E. Turpeinen, R. L., Pongracz, E., & Keiski, R. (2009). Catalytic activation of CO2: Use of secondary CO2 for the production of synthesis gas and for methanol synthesis over copper-based zirconia-containing catalysts. *Catalysis Today 144* , 318-323.

Sheffer, G., King, T., Gerstein, B., & Chu, P.-J. (1989). NMR studies of 65Cu and 133Cs in alkali-metal-promoted copper catalyst. *Journal of Catalysis 115* , 194-204.

Suh, Y.-W., Moon, S.-H., & Rhee, H.-K. (2000). Active sites in Cu/ZnO/ZrO2 catalysts for methanol synthesis from CO/H2. *Catalysis Today 63* , 447-452.

Sun, J. T., Metcalfe, I. S., & Sahibzada, M. (1999). Deactivation of Cu/ZnO/Al2O3 methanol synthesis catalyst by sintering. *Industrial & Engineering Chemisrty Research 38* , 3868-3872.

www.methanex.com/methanol/techsafetydata.htm. (n.d.).

Yu, J., Ge, Q., Fang, W., & Xu, H. (2011). Influence of calcination temperature on the efficiency of CaO promotion over CaO modified Pt/y-Al2O3 catalyst. *Applied Catalysis A: General 395* , 114-119.

Zhang, Y., Sun, Q., Deng, J., Wu, D., & Chen, S. (1997). A high activity Cu/ZnO/Al2O3 catalyst for methanol synthesis: Preparation and catalytic properties. *Applied catalysis A: General 158* , 105-120.

Zhang, Y., Zhou, Y., YianLi, Wang, Y., Xui, Y., & Wu, P. (2007). Effect of calcination temperature on catalytic properties of PtSnNa/ZSM-5 catalyst for propane dehydrogenation. *Catalysis Communication 8* , 1009-1016.

APPENDICES

Appendix A: Gas Chromatography Analysis Results for Liquid and Gas Samples

CCZ 1

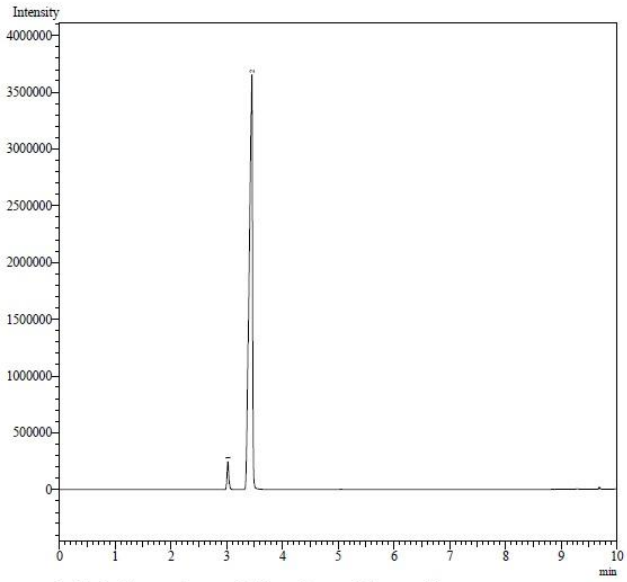

Peak#	Ret.Time	Area	Height	Conc.	Units	Name
1	3.0249	572805	244611	6.625	%	Methanol
2	3.4554	15049464	3647526	68.315	%	Ethanol
Total				74.940		

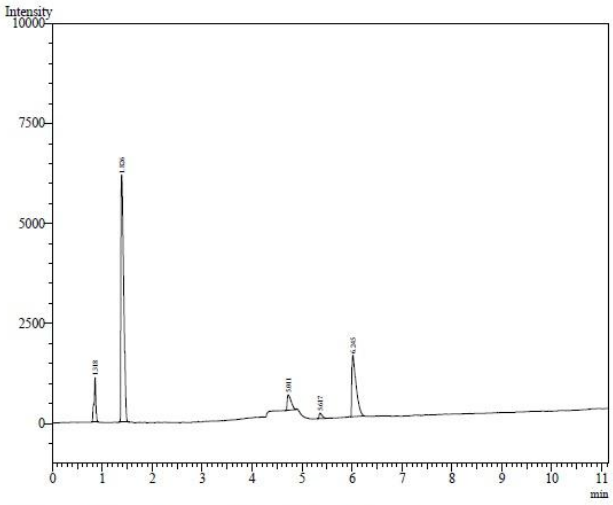

Peak#	Ret.Time	Area	Height	Conc.	Units	Name
1	1.318	2688.04	1104.70	3.0207	mole %	Air (N2 +O2)
2	1.826	22376.41	6175.95	20.9332	mole %	Carbon Dioxide
3	5.011	1999.85	387.39	0.0000		
4	5.617	540.47	142.70	0.0000		
5	6.245	8562.45	1536.55	0.0000		
Total		36167.22		23.9539		

CCZ 2

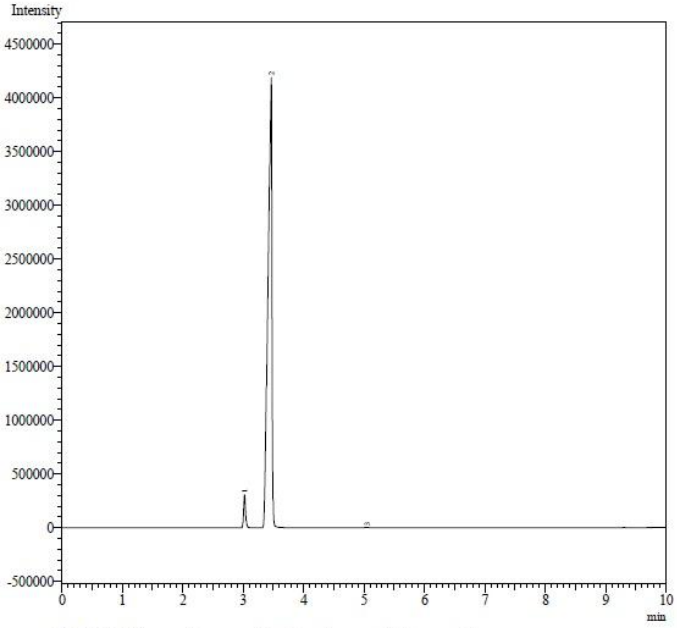

Peak#	Ret.Time	Area	Height	Conc.	Units	Name
1	3.0262	712336	304908	4.329	%	Methanol
2	3.4685	18878108	4182206	85.694	%	Ethanol
3	5.0456	10833	2994	0.000		
Total				90.024		

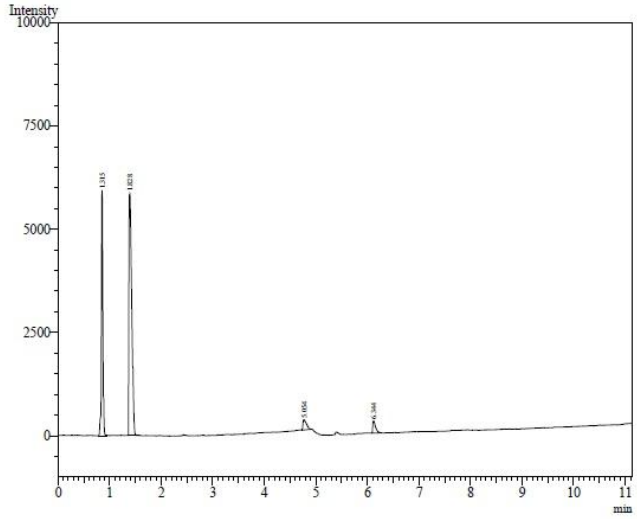

Peak#	Ret.Time	Area	Height	Conc.	Units	Name
1	1.315	11375.70	5924.03	0.0000	mole %	Air
2	1.828	20679.65	5871.22	19.3458	mole %	Carbon Dioxide
3	5.054	1122.42	248.77	0.0000		
4	6.344	1066.74	295.83	0.0000		
Total		34244.51		19.3458		

CCZ 3

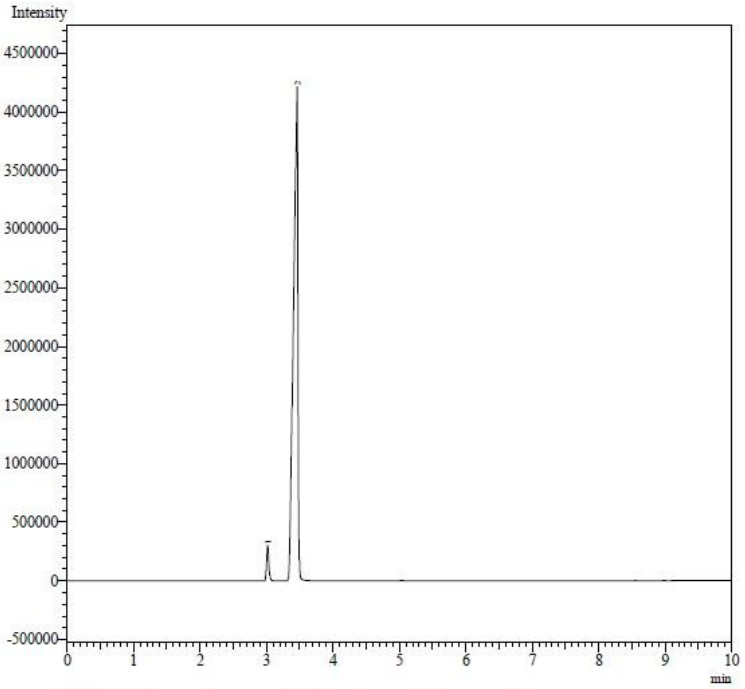

Peak#	Ret.Time	Area	Height	Conc.	Units	Name
1	3.0219	713955	303065	8.258	%	Methanol
2	3.4656	19255986	4202956	87.410	%	Ethanol
Total				95.668		

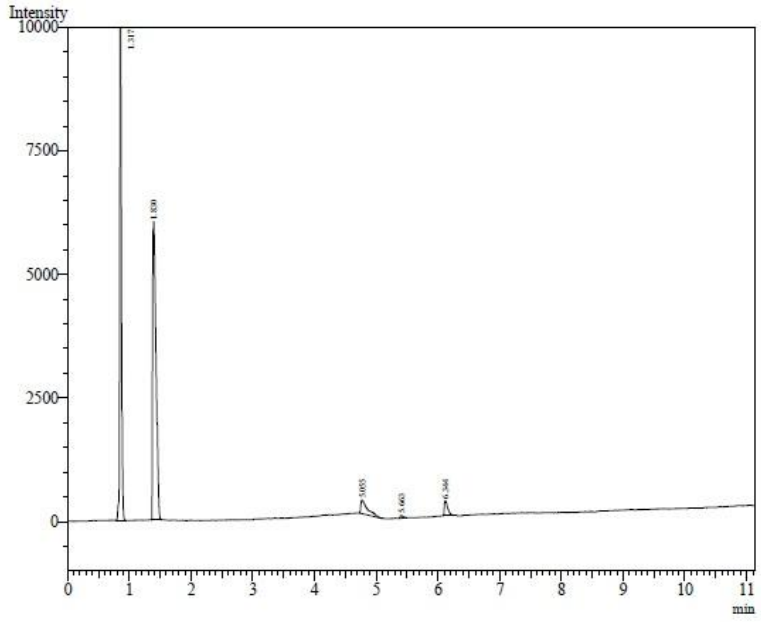

Peak#	Ret.Time	Area	Height	Conc.	Units	Name
1	1.317	19730.93	10474.23	0.0000	mole %	Air
2	1.830	21587.29	6017.78	20.1949	mole %	Carbon Dioxide
3	5.055	1999.26	276.23	0.0000		
4	5.663	166.63	55.17	0.0000		
5	6.344	1108.92	305.10	0.0000		
Total		44593.03		20.1949		

CCZ 4

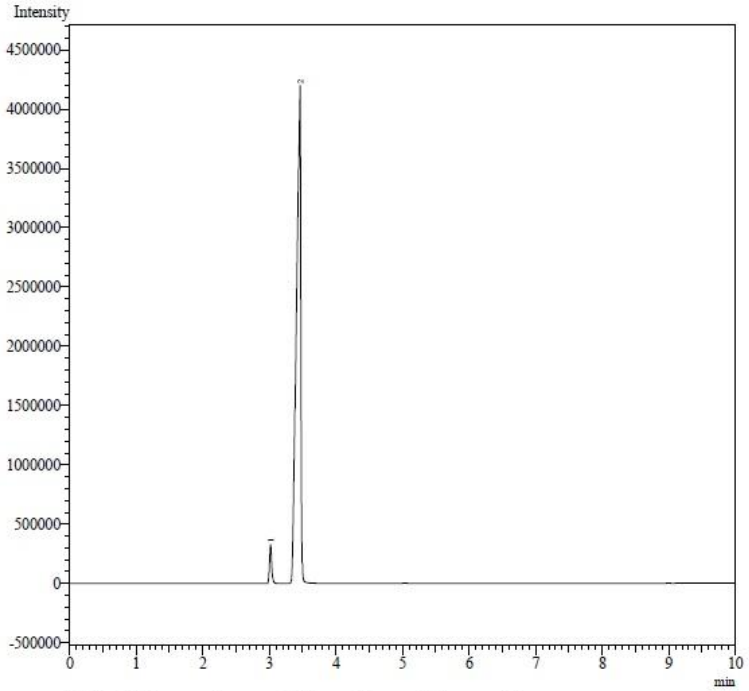

Peak#	Ret.Time	Area	Height	Conc.	Units	Name
1	3.0221	759115	324358	8.780	%	Methanol
2	3.4653	19065438	4190229	86.545	%	Ethanol
Total				95.325		

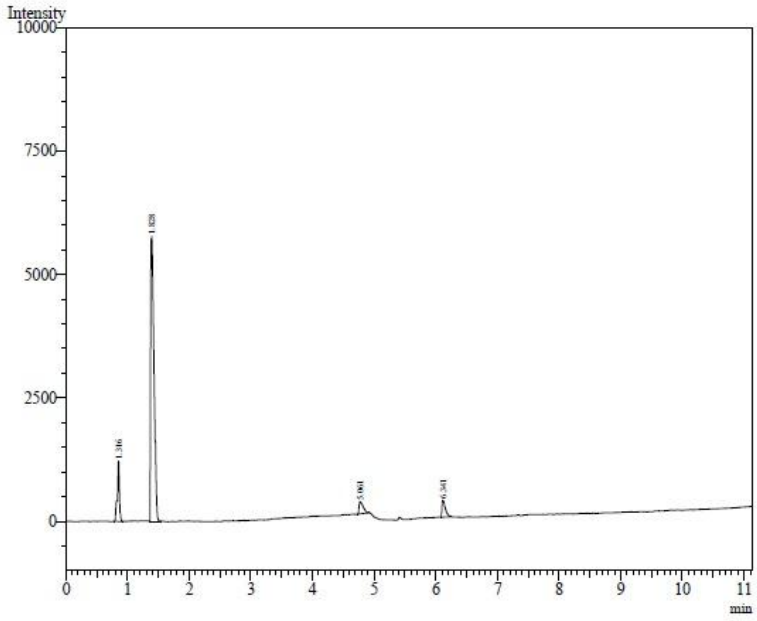

Peak#	Ret.Time	Area	Height	Conc.	Units	Name
1	1.316	2785.78	1216.05	3.1306	mole %	Air (N2 +O2)
2	1.828	20158.02	5771.66	18.8579	mole %	Carbon Dioxide
3	5.061	1098.47	245.74	0.0000		
4	6.341	1230.22	340.02	0.0000		
Total		25272.49		21.9884		

CCZ 5

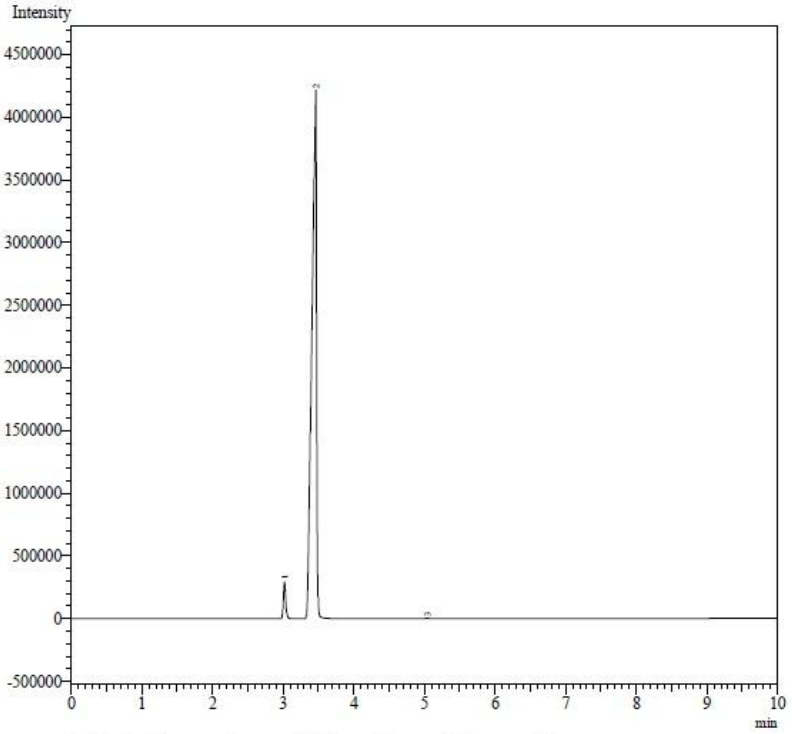

Peak#	Ret.Time	Area	Height	Conc.	Units	Name
1	3.0229	690104	290723	4.194	%	Methanol
2	3.4655	19238960	4203433	87.333	%	Ethanol
3	5.0405	10961	2993	0.000		
Total				91.527		

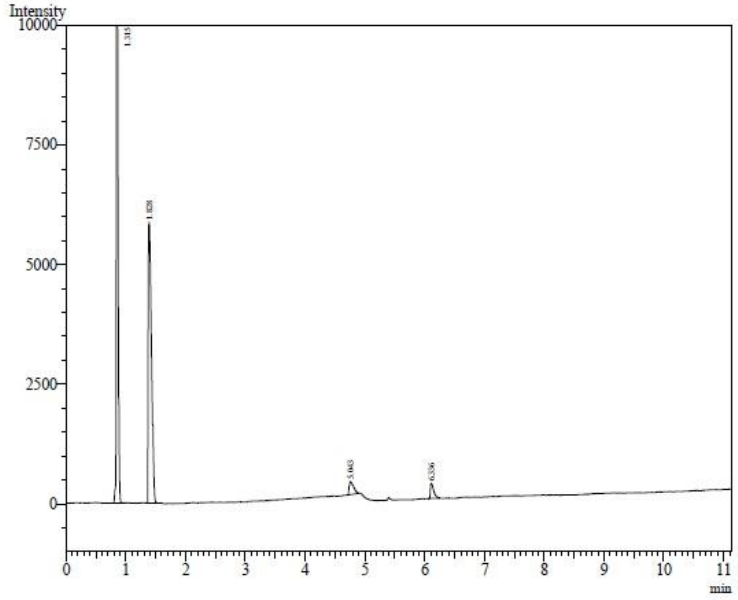

Peak#	Ret.Time	Area	Height	Conc.	Units	Name
1	1.315	24380.52	13266.19	0.0000	mole %	Air
2	1.828	20553.91	5867.27	19.2282	mole %	Carbon Dioxide
3	5.043	1294.75	267.49	0.0000		
4	6.336	1154.06	320.88	0.0000		
Total		47383.24		19.2282		

CCZ 6

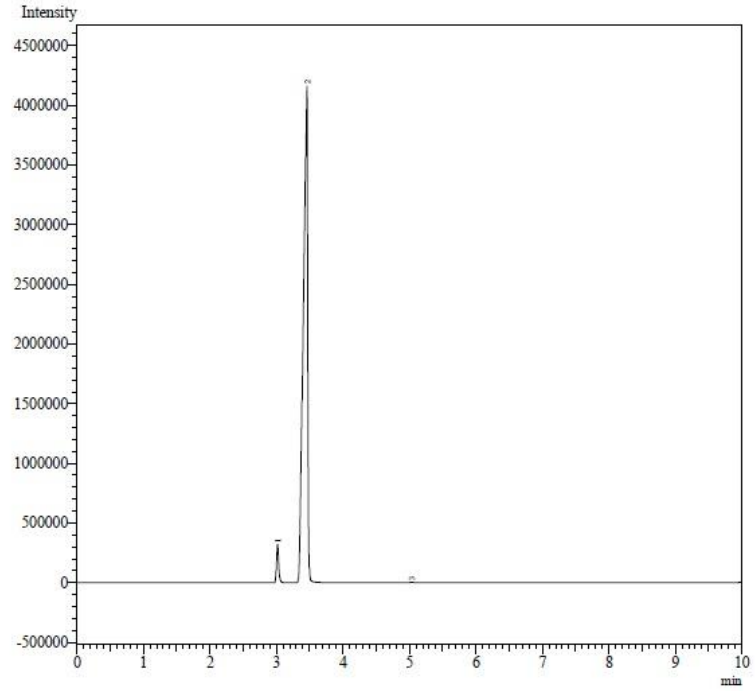

Peak#	Ret.Time	Area	Height	Conc.	Units	Name
1	3.0210	740367	318480	4.500	%	Methanol
2	3.4625	18709683	4143455	84.930	%	Ethanol
3	5.0365	10094	2685	0.000		
Total				89.430		

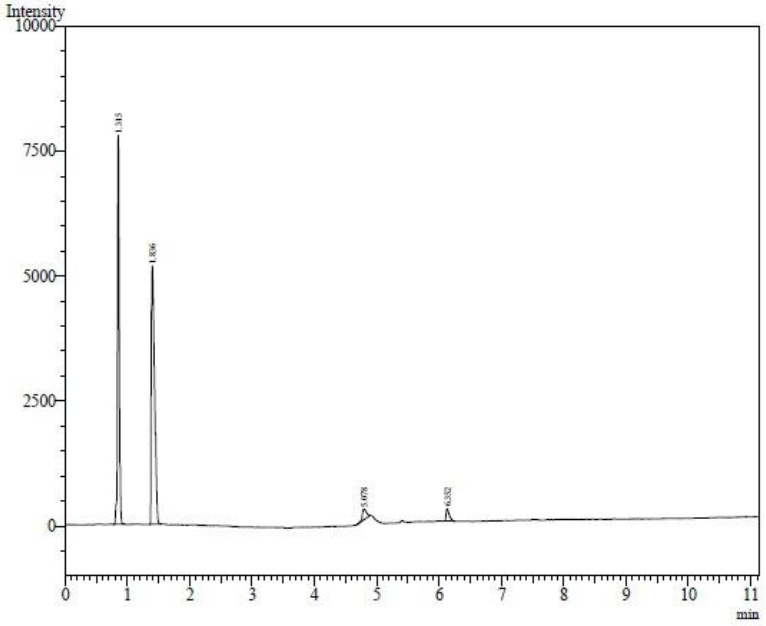

Peak#	Ret.Time	Area	Height	Conc.	Units	Name
1	1.315	14836.79	7762.31	0.0000	mole %	Air
2	1.836	17558.02	5164.18	16.4256	mole %	Carbon Dioxide
3	5.078	945.42	218.15	0.0000		
4	6.352	811.05	244.41	0.0000		
Total		34151.28		16.4256		

Feed Gas

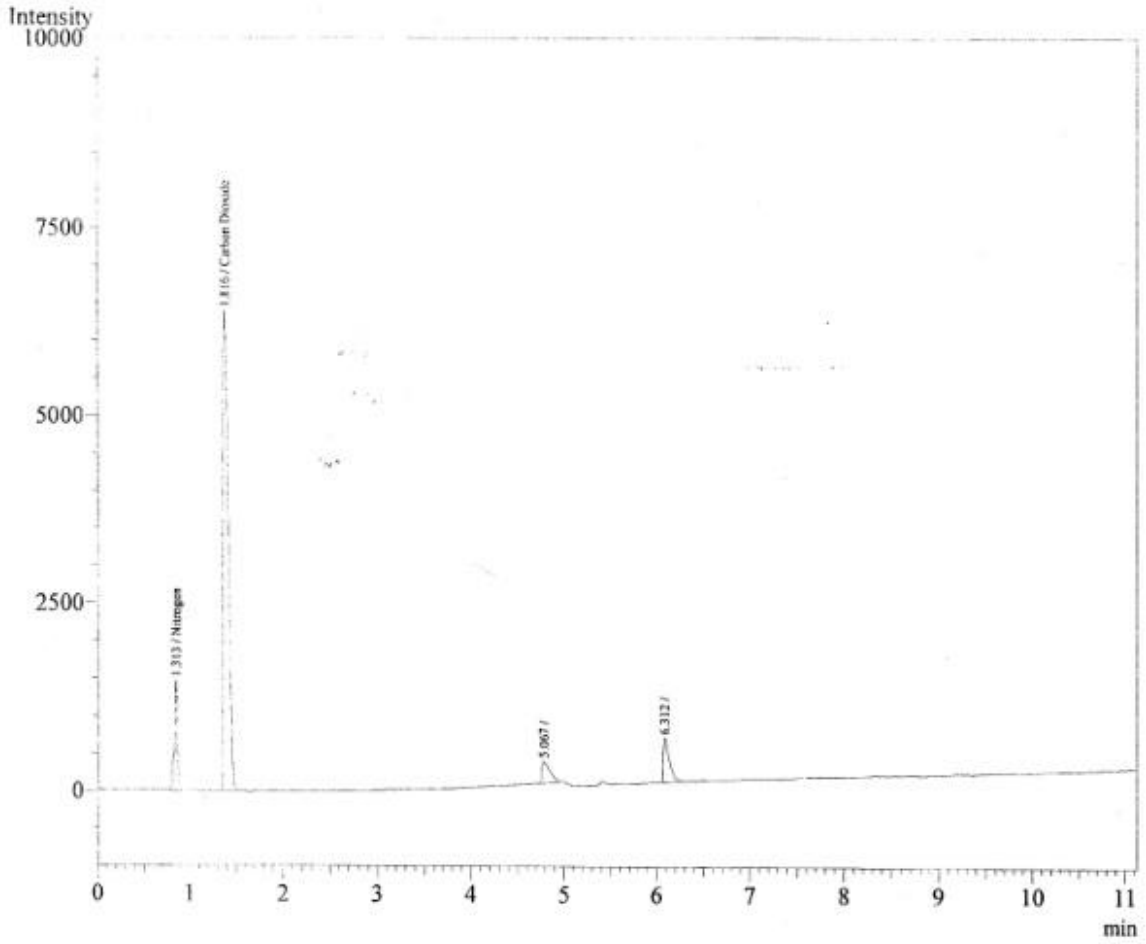

Peak#	Ret.Time	Area	Height	Conc.	Units	Name
1	1.313	3207.98	1452.16	3.6050	mole %	Nitrogen
2	1.816	23396.35	6370.94	21.8873	mole %	Carbon Dioxide
3	5.067	1604.15	290.93	0.0000		
4	6.312	2505.68	588.73	0.0000		
Total		30714.16		25.4923		

Appendix B: Summary Report of BET Analysis

CCZ 1

Summary Report

Surface Area

Single point surface area at p/p° = 0.300640924:	109.6533 m²/g
BET Surface Area:	111.2996 m²/g
Langmuir Surface Area:	164.6951 m²/g
t-Plot Micropore Area:	37.8003 m²/g
t-Plot External Surface Area:	73.4992 m²/g
BJH Adsorption cumulative surface area of pores between 17.000 Å and 3000.000 Å diameter:	54.357 m²/g
BJH Desorption cumulative surface area of pores between 17.000 Å and 3000.000 Å diameter:	68.2518 m²/g
D-H Adsorption cumulative surface area of pores between 17.000 Å and 3000.000 Å diameter:	57.785 m²/g
D-H Desorption cumulative surface area of pores between 17.000 Å and 3000.000 Å diameter:	58.1125 m²/g

Pore Volume

Single point adsorption total pore volume of pores less than 3113.100 Å diameter at p/p° = 0.993765284:	0.198296 cm³/g
t-Plot micropore volume:	0.019116 cm³/g
BJH Adsorption cumulative volume of pores between 17.000 Å and 3000.000 Å diameter:	0.164160 cm³/g
BJH Desorption cumulative volume of pores between 17.000 Å and 3000.000 Å diameter:	0.190064 cm³/g
D-H Adsorption cumulative volume of pores between 17.000 Å and 3000.000 Å diameter:	0.169545 cm³/g
D-H Desorption cumulative volume of pores between 17.000 Å and 3000.000 Å diameter:	0.181025 cm³/g

CCZ 2

Summary Report

Surface Area

Single point surface area at p/p° = 0.300689646:	67.7473 m²/g
BET Surface Area:	69.0478 m²/g
Langmuir Surface Area:	103.2722 m²/g
t-Plot Micropore Area:	14.6137 m²/g
t-Plot External Surface Area:	54.4341 m²/g
BJH Adsorption cumulative surface area of pores between 17.000 Å and 3000.000 Å diameter:	53.895 m²/g
BJH Desorption cumulative surface area of pores between 17.000 Å and 3000.000 Å diameter:	52.2407 m²/g
D-H Adsorption cumulative surface area of pores between 17.000 Å and 3000.000 Å diameter:	44.277 m²/g
D-H Desorption cumulative surface area of pores between 17.000 Å and 3000.000 Å diameter:	44.4747 m²/g

Pore Volume

Single point adsorption total pore volume of pores less than 3032.476 Å diameter at p/p° = 0.993597648:	0.132899 cm³/g
t-Plot micropore volume:	0.007261 cm³/g
BJH Adsorption cumulative volume of pores between 17.000 Å and 3000.000 Å diameter:	0.124620 cm³/g
BJH Desorption cumulative volume of pores between 17.000 Å and 3000.000 Å diameter:	0.139676 cm³/g
D-H Adsorption cumulative volume of pores between 17.000 Å and 3000.000 Å diameter:	0.118992 cm³/g
D-H Desorption cumulative volume of pores between 17.000 Å and 3000.000 Å diameter:	0.128433 cm³/g

CCZ 3

Summary Report

Surface Area

Single point surface area at p/p° = 0.299550817:	26.4349 m²/g
BET Surface Area:	27.1294 m²/g
Langmuir Surface Area:	41.7204 m²/g
t-Plot External Surface Area:	27.8838 m²/g
BJH Adsorption cumulative surface area of pores between 17.000 Å and 3000.000 Å diameter:	28.239 m²/g
BJH Desorption cumulative surface area of pores between 17.000 Å and 3000.000 Å diameter:	30.3030 m²/g
D-H Adsorption cumulative surface area of pores between 17.000 Å and 3000.000 Å diameter:	26.204 m²/g
D-H Desorption cumulative surface area of pores between 17.000 Å and 3000.000 Å diameter:	26.4691 m²/g

Pore Volume

Single point adsorption total pore volume of pores less than 3046.234 Å diameter at p/p° = 0.993626887:	0.099101 cm³/g
t-Plot micropore volume:	-0.000601 cm³/g
BJH Adsorption cumulative volume of pores between 17.000 Å and 3000.000 Å diameter:	0.097435 cm³/g
BJH Desorption cumulative volume of pores between 17.000 Å and 3000.000 Å diameter:	0.113200 cm³/g
D-H Adsorption cumulative volume of pores between 17.000 Å and 3000.000 Å diameter:	0.097630 cm³/g
D-H Desorption cumulative volume of pores between 17.000 Å and 3000.000 Å diameter:	0.105322 cm³/g

Pore Size

Adsorption average pore width (4V/A by BET):	146.1158 Å

CCZ 4

Summary Report

Surface Area

Single point surface area at p/p° = 0.299736699:	11.5618 m²/g
BET Surface Area:	11.8734 m²/g
Langmuir Surface Area:	18.1005 m²/g
t-Plot Micropore Area:	1.1086 m²/g
t-Plot External Surface Area:	10.7648 m²/g
BJH Adsorption cumulative surface area of pores between 17.000 Å and 3000.000 Å diameter:	9.611 m²/g
BJH Desorption cumulative surface area of pores between 17.000 Å and 3000.000 Å diameter:	10.5807 m²/g
D-H Adsorption cumulative surface area of pores between 17.000 Å and 3000.000 Å diameter:	8.696 m²/g
D-H Desorption cumulative surface area of pores between 17.000 Å and 3000.000 Å diameter:	8.9331 m²/g

Pore Volume

Single point adsorption total pore volume of pores less than 3191.406 Å diameter at p/p° = 0.993919924:	0.049217 cm³/g
t-Plot micropore volume:	0.000510 cm³/g
BJH Adsorption cumulative volume of pores between 17.000 Å and 3000.000 Å diameter:	0.047650 cm³/g
BJH Desorption cumulative volume of pores between 17.000 Å and 3000.000 Å diameter:	0.057276 cm³/g
D-H Adsorption cumulative volume of pores between 17.000 Å and 3000.000 Å diameter:	0.047397 cm³/g
D-H Desorption cumulative volume of pores between 17.000 Å and 3000.000 Å diameter:	0.051008 cm³/g

CCZ 5

Summary Report

Surface Area

Single point surface area at P/Po = 0.248277244:	140.1143 m²/g
BET Surface Area:	140.5712 m²/g
Langmuir Surface Area:	200.8539 m²/g
t-Plot Micropore Area:	51.6285 m²/g
t-Plot External Surface Area:	88.9427 m²/g
BJH Adsorption cumulative surface area of pores between 17.000 Å and 3000.000 Å width:	76.487 m²/g
BJH Desorption cumulative surface area of pores between 17.000 Å and 3000.000 Å width:	81.6595 m²/g

Pore Volume

Single point adsorption total pore volume of pores less than 1255.583 Å width at P/Po = 0.984338141:	0.193459 cm³/g
Single point desorption total pore volume of pores less than 1014.492 Å width at P/Po = 0.980536632:	0.207077 cm³/g
t-Plot micropore volume:	0.024818 cm³/g
BJH Adsorption cumulative volume of pores between 17.000 Å and 3000.000 Å width:	0.185768 cm³/g
BJH Desorption cumulative volume of pores between 17.000 Å and 3000.000 Å width:	0.187830 cm³/g

Pore Size

Adsorption average pore width (4V/A by BET):	55.0495 Å
Desorption average pore width (4V/A by BET):	58.9245 Å
BJH Adsorption average pore width (4V/A):	97.150 Å
BJH Desorption average pore width (4V/A):	92.006 Å

CCZ 6

Summary Report

Surface Area

Single point surface area at P/Po = 0.249771474:	18.9080 m²/g
BET Surface Area:	19.6666 m²/g
Langmuir Surface Area:	29.4137 m²/g
t-Plot External Surface Area:	20.1246 m²/g
BJH Adsorption cumulative surface area of pores between 17.000 Å and 3000.000 Å width:	21.282 m²/g
BJH Desorption cumulative surface area of pores between 17.000 Å and 3000.000 Å width:	22.1366 m²/g

Pore Volume

Single point adsorption total pore volume of pores less than 1196.344 Å width at P/Po = 0.983547989:	0.059071 cm³/g
Single point desorption total pore volume of pores less than 945.596 Å width at P/Po = 0.979088266:	0.065223 cm³/g
t-Plot micropore volume:	-0.000480 cm³/g
BJH Adsorption cumulative volume of pores between 17.000 Å and 3000.000 Å width:	0.070807 cm³/g
BJH Desorption cumulative volume of pores between 17.000 Å and 3000.000 Å width:	0.070586 cm³/g

Pore Size

Adsorption average pore width (4V/A by BET):	120.1455 Å
Desorption average pore width (4V/A by BET):	132.6567 Å
BJH Adsorption average pore width (4V/A):	133.086 Å
BJH Desorption average pore width (4V/A):	127.546 Å

Appendix C:Calculation for $CU(NO_3)_2.3H_2O$ and $Zr(NO_3)_4.6H_2O$ needed in preparing catalyst with 20wt % of Cu and 5wt% of Zr both deposited on CNF

Y=Mass of Cu

Z=Mass of Zr

Molar mass of $CU(NO_3)_2.3H_2O$=241.60 g/mol

Molar mass of $Zr(NO_3)_4.6H_2O$=231.23 g/mol

Molar mass of Cu=63.546 g/mol

Molar mass of Zr=91.22 g/mol

- Mass of Cu and Zr deposited on the CNF

$$\frac{Mass\ of\ component}{Total\ mass\ of\ catalyst} \times 100\%$$

- Mass of 20wt% Cu that deposited on the CNF

$$\frac{y}{1+z+y} \times 100 = 20\%$$

$$y = 0.2 + 0.2z + 0.2y$$

- Mass of 5wt% Zr that deposited on the CNF

$$\frac{z}{1+z+y} \times 100 = 5\%$$

$$z = 0.05 + 0.05z + 0.05y$$

Solve simultaneously 1 and 2

$$0.8y = 0.2 + 0.2z$$

$$0.95z = 0.05 + 0.05y$$

$$0.8y = 0.2 + 0.2z$$

$$0.8y = -0.8 + 15.2z$$

$$z = \frac{1}{15}$$

$$0.8y = 0.2 + 0.2(\frac{1}{15})$$

$$y = 0.2666$$

- Moles of Cu present in the catalyst

$$\frac{0.2666\ g}{63.546\ g/mol} = 4.1954 \times 10^{-3}$$

- Mass of $Cu(NO_3)_2.3H_2O$ needed

$$241.60\ g/mol\ \times\ 4.1954 \times 10^{-3} = 1.0136\ g$$

- Moles of Zr present in the catalyst

$$\frac{0.0666\ g}{123.22\ g/mol} = 5.4098 \times 10^{-4}$$

- Mass of $Zr(NO_3)_4.6H_2O$ needed

$$231.23\ g/mol\ \times 5.4098 \times 10^{-4} = 0.1251\ g$$